



A cascade of sulfur transferases delivers sulfur to the sulfur-oxidizing heterodisulfide reductase-like complex

Tomohisa Sebastian Tanabe^{1,2}  | Elena Bach¹ | Giulia D'Ermo³ |
 Marc Gregor Mohr¹ | Natalie Hager¹ | Niklas Pfeiffer¹ | Marianne Guiral³ |
 Christiane Dahl¹ 

¹Institut für Mikrobiologie & Biotechnologie, Rheinische Friedrich-Wilhelms-Universität Bonn, Bonn, Germany

²Division of Microbial Ecology, University of Vienna, Wien, Austria

³CNRS, Bioénergétique et Ingénierie des Protéines, Aix Marseille Université, IMM, Marseille, France

Correspondence

Christiane Dahl, Institut für Mikrobiologie & Biotechnologie, Rheinische Friedrich-Wilhelms-Universität Bonn, Meckenheimer Allee 168, D-53115 Bonn, Germany.
 Email: chdahl@uni-bonn.de

Present addresses

Tomohisa Sebastian Tanabe, Division of Microbial Ecology, University of Vienna, Djerassiplatz 1, A-1030 Wien, Köln, Austria; and Niklas Pfeiffer, Labor Dr. Wisplinghoff, Horbeller Str. 18-20, Köln, Germany.

Funding information

Deutscher Akademischer Austauschdienst/Hubert Curien Procope program, Grant/Award Numbers: 57388731, 40444VM; Studienstiftung des Deutschen Volkes; Deutsche Forschungsgemeinschaft, Grant/Award Number: 351/13-1

Review Editor: John Kuriyan

Abstract

A heterodisulfide reductase-like complex (sHdr) and novel lipoate-binding proteins (LbpAs) are central players of a wide-spread pathway of dissimilatory sulfur oxidation. Bioinformatic analysis demonstrate that the cytoplasmic sHdr-LbpA systems are always accompanied by sets of sulfur transferases (DsrE proteins, TusA, and rhodanases). The exact composition of these sets may vary depending on the organism and sHdr system type. To enable generalizations, we studied model sulfur oxidizers from distant bacterial phyla, that is, Aquificota and Pseudomonadota. DsrE3C of the chemoorganotrophic Alphaproteobacterium *Hyphomicrobium denitrificans* and DsrE3B from the Gammaproteobacteria *Thioalkalivibrio* sp. K90mix, an obligate chemolithotroph, and *Thiorhodospira sibirica*, an obligate photolithotroph, are homotrimers that donate sulfur to TusA. Additionally, the hypomicrobial rhodanese-like protein Rhd442 exchanges sulfur with both TusA and DsrE3C. The latter is essential for sulfur oxidation in *Hm. denitrificans*. TusA from *Aquifex aeolicus* (AqTusA) interacts physiologically with AqDsrE, AqLbpA, and AqsHdr proteins. This is particularly significant as it establishes a direct link between sulfur transferases and the sHdr-LbpA complex that oxidizes sulfane sulfur to sulfite. In vivo, it is unlikely that there is a strict unidirectional transfer between the sulfur-binding enzymes studied. Rather, the sulfur transferases form a network, each with a pool of bound sulfur. Sulfur flux can then be shifted in one direction or the other depending on metabolic requirements. A single pair of sulfur-binding proteins with a preferred transfer direction, such as a DsrE3-type protein towards TusA, may be sufficient to push sulfur into the sink where it is further metabolized or needed.

KEYWORDS

Aquifex aeolicus, dissimilatory sulfur oxidation, DsrE, sHdr pathway, sulfur transferases

1 | INTRODUCTION

In the cytoplasm of prokaryotes, as in most (if not all) other biological contexts, reduced sulfur is normally handled in a protein-bound state due to its reactivity (Dahl, 2015; Gojon, 2020; Kessler, 2006; Mueller, 2006; Tanabe et al., 2019). Often, multiple sulfur transferases form a network to direct the sulfur to the correct metabolic pipeline or its target molecule. In these networks, individual sulfur-trafficking proteins may provide sulfur to multiple target reactions/proteins. Such networks are not only important for the biosynthesis of sulfur-containing cellular components but also essential in many bacteria and archaea, which carry out dissimilatory sulfur oxidation with energy conservation via respiratory or photosynthetic electron transport (Dahl, 2017; Dahl, 2020). Here, the enzymatic production of persulfide sulfur, the successive transfer of sulfur as a persulfide between multiple proteins, and the oxidation of sulfane sulfur in protein-bound form are all crucial steps. Rhodanases, TusA, and DsrE-like sulfur transferases are central and common elements in these processes. They have an established role in the rDsr pathway of sulfur oxidation where they work together to transfer sulfur as a cysteine persulfide to DsrC, which ultimately presents the sulfur to the oxidizing enzymatic unit, dissimilatory sulfite reductase, DsrAB (Dahl, 2020; Stockdreher et al., 2012, 2014). In the model organism *Allochromatium vinosum*, sulfur atoms are successively transferred from the rhodanase Rhd_2599 to TusA (Stockdreher et al., 2014), then to a conserved cysteine residue of DsrE, the active site subunit of the heterohexameric DsrE₂F₂H₂ complex (Dahl et al., 2008), and from there to DsrC (Stockdreher et al., 2012). The function of the AvDsrE2A protein, another sulfur transferase involved in this enzymatic relay, remains unclear (Stockdreher et al., 2014).

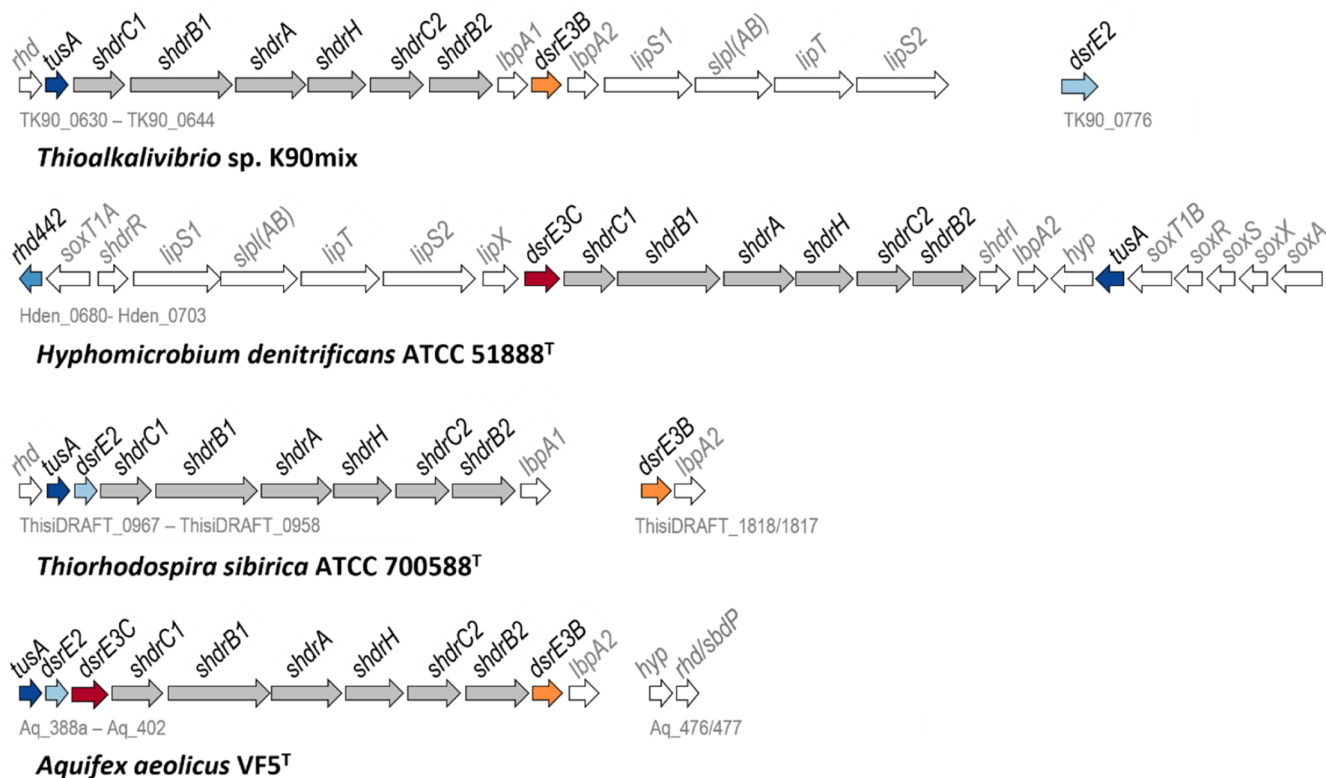
Recently, the sulfur-oxidizing heterodisulfide reductase-like sHdr complex and novel lipoate-binding proteins (LbpAs) have been identified as central players of an additional widespread sulfur oxidation pathway (Cao et al., 2018; Koch & Dahl, 2018; Tanabe et al., 2023). The sHdr–LbpA system exists in a significant group of organisms that comprise the volatile organic sulfur compound degrader *Hyphomicrobium denitrificans*, along with many chemo- and photolithoautotrophic bacteria and archaea, that include several environmentally relevant sulfur oxidizers, such as *Acidithiobacillus* sp., *Thioalkalivibrio* or *Sulfobacillus* species, and the hyperthermophile *Aquifex aeolicus*. Two types of *shdr* gene clusters can be differentiated (Figure 1): Type I with an *shdrC1B1AHC2B2* arrangement and type II with an

shdrC1B1AHB3-ETFAB-emo arrangement (Cao et al., 2018; Justice et al., 2014; Kümpel et al., 2024). Based on the copurification of sHdrA, B1, B2, C1, and C2 from *Aq. aeolicus* (Boughanemi et al., 2016), the crystal structure of the sHdrA homodimer from *Hm. denitrificans* (Ernst et al., 2021), and the heterohexameric HdrA₂B₂C₂ structure of the heterodisulfide reductase from methanogenic archaea (Wagner et al., 2017), a sHdrAA'C1B1C2B2 stoichiometry was predicted for the type I sHdr complex from sulfur oxidizers (Ernst et al., 2021). Type II sHdr complexes are proposed to have a similar composition with sHdrC2B2 being replaced by sHdrB3, which is essentially a fusion of the former two subunits (Kümpel et al., 2024). While the importance of the type I system for sulfur dissimilation has been proven (Cao et al., 2018; Koch & Dahl, 2018; Tanabe et al., 2023), less is known for type II, although prokaryotes encoding the type II system are known sulfur oxidizers (Justice et al., 2014). Irrespective of the type of gene cluster, the *shdr-lbpA* genes are conspicuously often associated with genes for accessory sulfur transferases similar to but not identical with those that fuel the rDsr pathway (Figure 1) (Cao et al., 2018; Koch & Dahl, 2018).

Biochemical information regarding sulfur transferases associated with sHdr is extremely limited. The only sHdr-associated sulfur transferases studied thus far come from the archaeon *Metallospira cuprina*. Its DsrE3A protein has been biochemically characterized as a thiosulfonate transferase (Liu et al., 2014). Bound thiosulfate is transferred from DsrE3A to TusA but not vice versa (Liu et al., 2014) implying that DsrE3A functions as a thiosulfate donor to TusA in vivo. The DsrE2A-type sulfur transferases, which are encoded in certain *shdr* gene clusters (Figure 1), have been proposed as potential membrane anchors for the sHdr-like complex (Boughanemi et al., 2016).

Here we set out to shed more light on sulfur transfer to the sHdr system. Initially, we analyze the potential correlation between the prevalence of *shdr* and sulfur transferase genes. To enable generalizations, we concentrate on the type I sHdr system in bacteria and our model organisms stem from two distant phyla: the Aquificota (*Aquifex aeolicus*) and the Pseudomonadota, which are represented by sulfur oxidizers from two different classes, the Alphaproteobacteria (*Hyphomicrobium denitrificans*) and the Gammaproteobacteria (*Thiorhodospira sibirica* and *Thioalkalivibrio* sp. K90mix). From these organisms, we investigate the proteins Rhd442, TusA, DsrE3B, and DsrE3C to determine whether and how they mobilize and transfer sulfur. In the genetically accessible *Hm. denitrificans*, we gather information on the importance of DsrE3C in vivo.

Type I sHdr system



Type II sHdr system

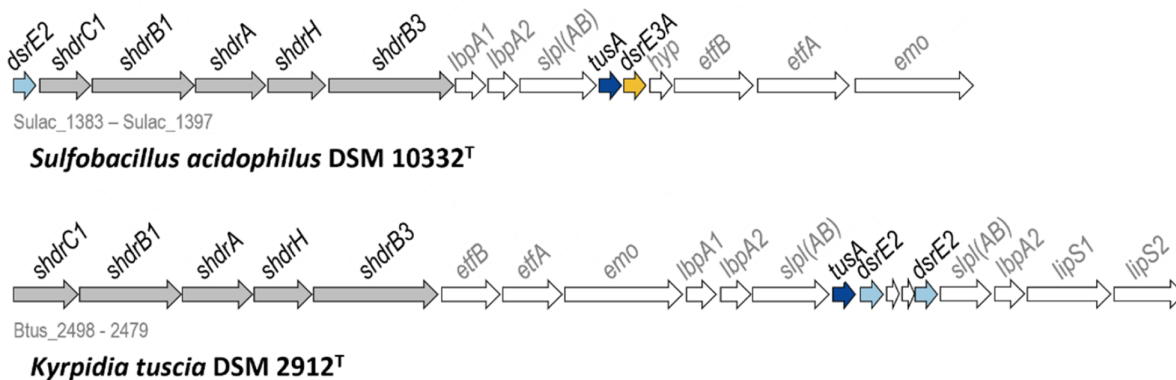


FIGURE 1 Representative *shdr* gene clusters in sulfur oxidizers. The KEGG/NCBI locus tag identifiers for the first and last genes are shown below each cluster. For *Ts. sibirica*, locus tags are given according to JGI IMG. Genes for Tusa, DsrE2, DsrE3A, DsrE3B, and DsrE3C are indicated in dark blue, light blue, yellow, orange, and dark red, respectively. Genes for probable components of the sulfur-oxidizing heterodisulfide reductase-like (sHdr) complex are shaded in gray. EMO, ETF:(methyl)menaquinone oxidoreductase; Etf, electron transfer protein. EtfAB and EMO have been proposed to direct electrons stemming from sulfane sulfur oxidation to menaquinone (Kümpel et al., 2024). LbpA, lipoate-binding protein; sLp/(AB), lipoate: protein ligase; LipS1/S2, lipoyl synthase; LipT, FAD-binding NAD(P)H-dependent oxidoreductase possibly delivering electrons for the LipS1/S2-catalyzed sulfur insertion step (Kümpel et al., 2024; Tanabe et al., 2023); Rhd, rhodanese; SbdP, sulfur-binding-donating protein.

2 | RESULTS

2.1 | Distribution of the sHdr system

Clusters of genes encoding the sHdr pathway for sulfane sulfur oxidation in the cytoplasm fall into two distinct

categories (Cao et al., 2018; Justice et al., 2014; Kümpel et al., 2024) (Figures 1 and 2). The type I and type II sHdr systems share several core proteins, namely the Fe/S-flavoprotein sHdrA, the electron carrier protein sHdrC1, that binds two cubane [4Fe-4S] clusters and the proposed catalytic subunit sHdrB1 that probably

Treescale: 1

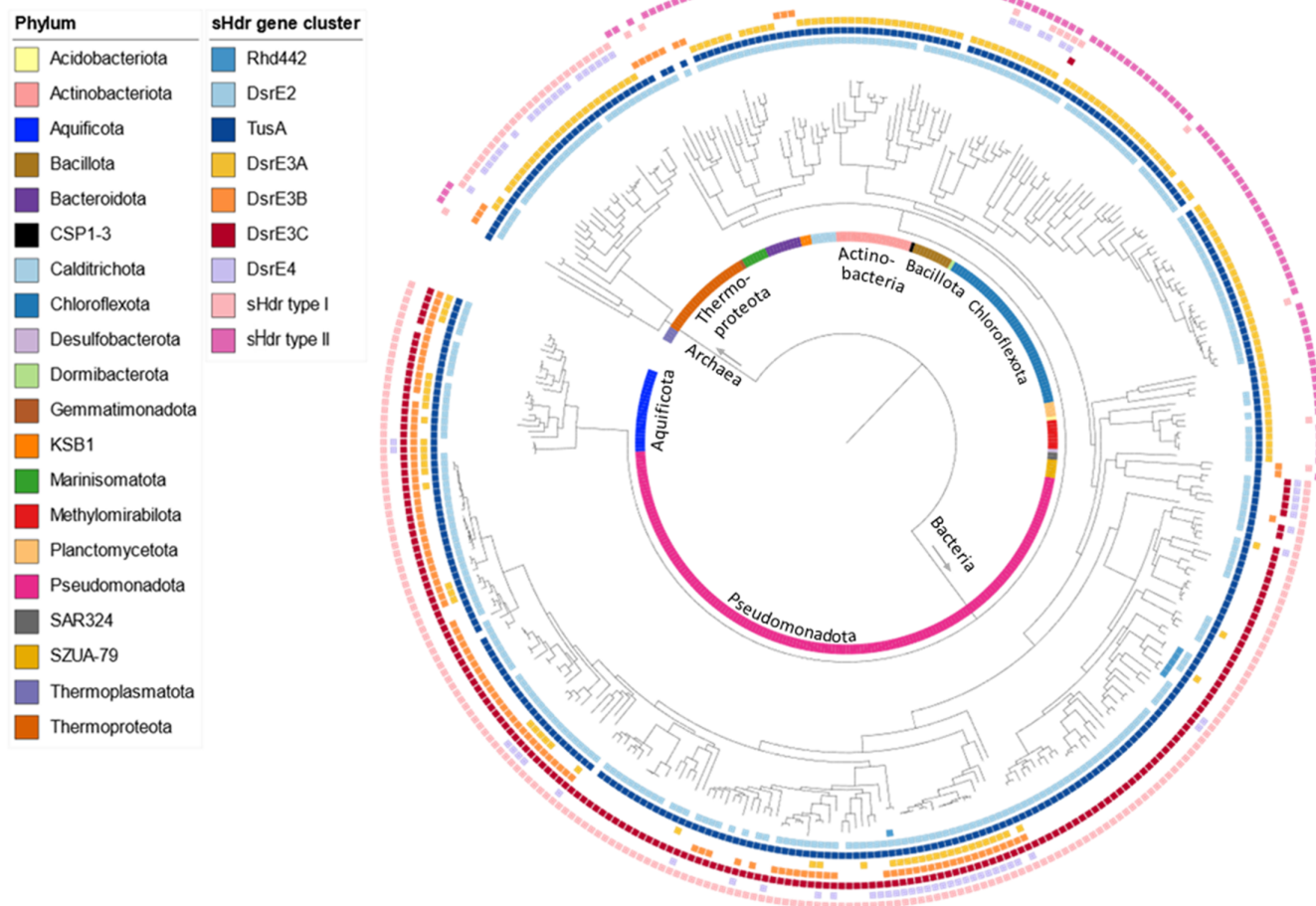


FIGURE 2 Taxonomic distribution of type I or type II sHdr systems in sulfur-oxidizing prokaryotes. The distribution of TusA, Rhd442, and DsrE-type sulfur transferases is also visualized. The data underlying the figure is provided in Table S1.

coordinates two noncubane Fe/S clusters (Ernst et al., 2021). sHdrC2 is another ferredoxin-like electron carrier. sHdrB2 has the potential to bind two classical noncubane Fe/S clusters and probably acts as a disulfide reductase (Ernst et al., 2021). Organisms with type II sHdr systems encode a protein that we term sHdrB3. This is a fusion of sHdrC2 and sHdrB2, albeit it can bind only one noncubane Fe/S cluster (Kümpel et al., 2024). Electron transfer protein EtfAB and ETF:(methyl)menaquinone oxidoreductase EMO are encoded within type II sHdr clusters and have been proposed to direct electrons stemming from sulfane sulfur oxidation to menaquinone (Kümpel et al., 2024).

Of the entire GTDB representative genome collection (release R207), 397 assemblies from 20 phyla contain core sHdr genes. For 353 of these assemblies, the concatenated sequences for 16 ribosomal proteins could be used as phylogenetic markers to compute a species tree (Hug et al., 2013; Jaffe et al., 2020), that served as the basis for mapping the distribution of type I and II

sHdr systems using HMSS2 (Tanabe & Dahl, 2023) (Figure 2, Table S1). Among the Bacteria, the Pseudomonadota, the Aquificota, and the phylum SZUA-79 have exclusively the type I system. Among the Archaea, the type I sHdr gene set occurs in the Thermoproteota, a phylum harboring well-established sulfur oxidizers like *Sulfolobus* sp. and *Acidianus* sp. The type II sHdr system is found in 130 assemblies from one archaeal and 12 bacterial phyla. The majority of the respective bacterial assemblies belong to the Chloroflexota, Actinobacteriota, and Bacillota. In some bacterial phyla, there are species that have either type I or type II sHdr systems (e.g., Marinisomatota or Chloroflexota). All sHdr-containing members of the Bacillota contain the type II system. In addition, four *Sulfobacillus* species, which are well-established sulfur oxidizers (Justice et al., 2014; Norris et al., 1996; Watanabe et al., 2019; Zhang et al., 2017), and one further member of the order Sulfo- bacillales bear the genetic capacity for both sHdr systems (Figure 2, Table S1).

2.2 | Distribution of sHdr-associated sulfur transferases

Here, we intended to further illuminate the general association of *shdr* gene clusters with genes for different sulfur transferases (Cao et al., 2018; Dahl, 2015; Kümpel et al., 2024; Liu et al., 2014) (TusA, DsrE-type sulfur transferases, rhodanese Rhd442). In order to do so, we first needed to clearly describe and validate the various classes of proteins using sequence similarity networks (SSN). Clusters in SSNs reflect phylogenetic clades (Atkinson et al., 2009).

TusA family proteins are a central hub in sulfur transfer during various anabolic and catabolic processes (Tanabe et al., 2019). In *Escherichia coli*, the three homologous TusA-family proteins, TusA, YedF, and YeeD have distinct functions and cannot substitute for each other (Dahl et al., 2013). Besides contributing to tRNA thiolation (Ikeuchi et al., 2006), TusA mediates sulfur transfer for molybdenum cofactor biosynthesis

and affects iron–sulfur cluster assembly as well as the activity of major regulatory proteins (Dahl et al., 2013; Ishii et al., 2000; Yildiz & Leimkühler, 2021). YeeD is a component of thiosulfate uptake for sulfur assimilation (Ikei et al., 2024; Tanaka et al., 2020). YedF in some way affects flagella formation and motility (Balleste-Delpierre et al., 2017). We retrieved all sequences clustering with these three proteins from Uniprot and subjected them to a SSN analysis together with TusA-like proteins that are genetically linked with sulfur-oxidation systems. Indeed, TusA, YedF, and YeeD each form distinct clusters of similar sequences (Figure 3a). In addition, three further clusters are clearly discernible. Two of them consist of TusA-like proteins linked with rDsr systems and a third comprises TusAs linked with sHdr and rDsr systems. In summary, TusAs genetically associated with sulfur oxidation systems can be confidently distinguished from classical TusA, YedF, and YeeD and form distinct phylogenetic clades (Figure 3a).

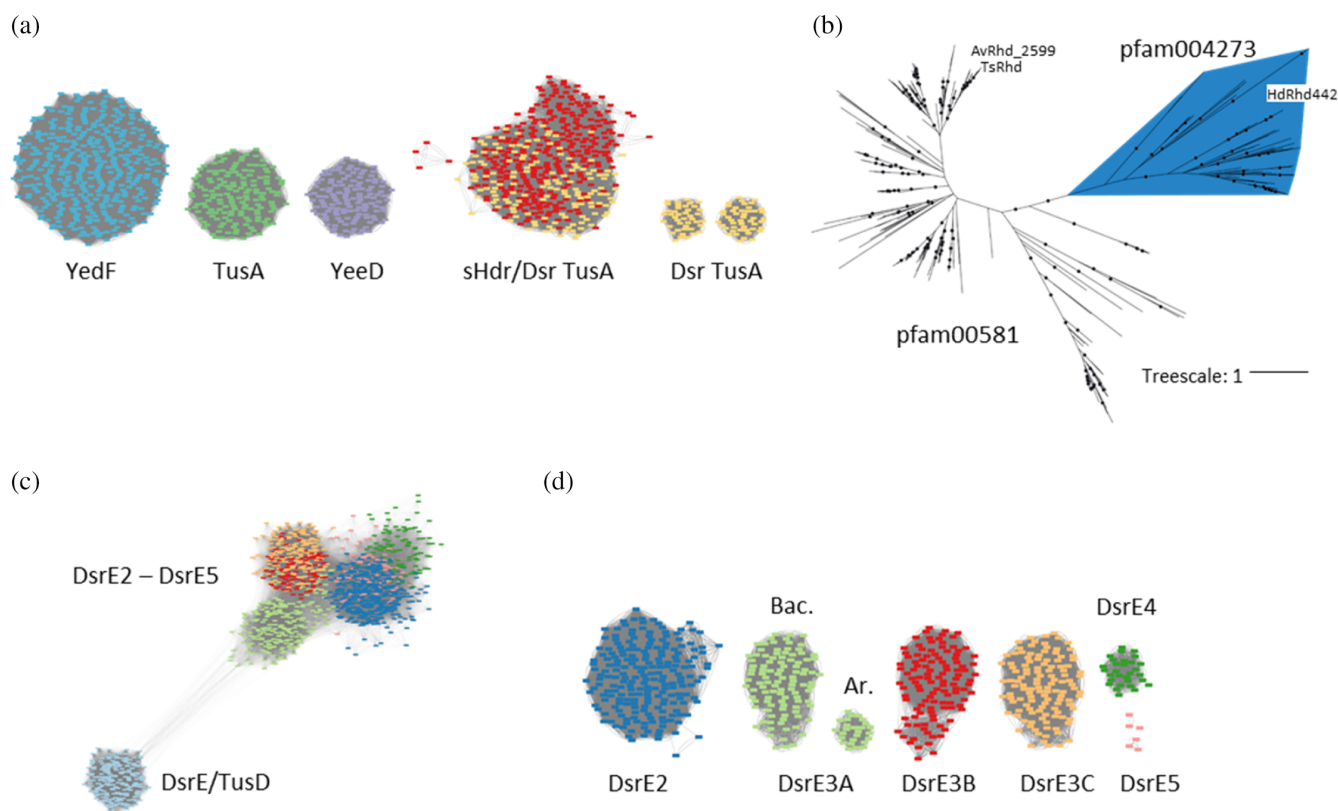


FIGURE 3 Sequence similarity network (SSN) and phylogenetic analyses for sulfur transferases relevant for dissimilatory sulfur oxidation. (a) SSN for the TusA family (pfam01206) members clustering at 50% identity with TusA, YedF, and YeeD from *E. coli* and TusA-like proteins that are genetically linked with sHdr and/or Dsr sulfur-oxidation systems. Connections below a threshold score of 100 were removed. (b) Maximum likelihood tree for ~100-aa single domain rhodanases that are encoded in synteny with DsrE2 and TusA or that are related to Rhd442 from *Hm. denitrificans* X^T. Bootstrap values exceeding 95% are indicated by dots. (c) SSN for all DsrE-type sequences from the representative genomes of GTDB (release R207). (d) SSN for all DsrE homologs associated with rDsr and/or sHdr systems, excluding the divergent TusD/DsrE proteins. Connections below a threshold score of 135 were removed. Ar, Archaea; Bac., Bacteria.

Rhodanases were originally identified and named on the basis of their ability to catalyze the transfer of a sulfane sulfur atom from thiosulfate to cyanide yielding SCN^- (rhodanide, thiocyanate) as the product (Westley, 1973). Rhodanases and rhodanase-like proteins are very widespread (Bordo & Bork, 2002) and therefore we did not consider it useful to create an SSN analysis spanning all prokaryotes, but instead limited ourselves to sulfur oxidizers with rDsr and/or sHdr systems. Within a first group of these, the corresponding gene is present in a syntenic cluster with genes for DsrE2 and TusA (e.g., in *Ts. sibirica*, Figure 1). A second group contains proteins related to rhodanase Rhd442 encoded in the vicinity of the *shdr* gene cluster in *Hm. denitrificans* X^T (Figure 1). By establishing a phylogenetic tree (Figure 3b), it became apparent that the DsrE2-TusA associated rhodanases belong to a different clade than the Rhd442-related proteins (Figure 3b). The former belong to a protein family (pfam00581) that also encompasses Rhd_2599 from *Ac. vinosum* (Stockdreher et al., 2014) and SbdP from *Aq. aeolicus* (Aussignargues et al., 2012). While the first is part of the relay delivering sulfur to the rDsr pathway of sulfur oxidation (Stockdreher et al., 2014), SbdP can load long sulfur chains and interacts with sulfur reductase and sulfur oxygenase reductase, that is, key enzymes of sulfur energy metabolism (Aussignargues et al., 2012). Rhd442 belongs to a separate protein family, pfam004273 (DUF442) that forms a monophyletic group in the rhodanase tree presented in Figure 3b.

Originally, the DsrE family has been categorized into five well distinguishable phylogenetic groups, DsrE, DsrE2, DsrE3 (with subgroups DsrE3A, DsrE3B, and DsrE3C), DsrE4, and DsrE5 (Boughanemi et al., 2016; Liu et al., 2014; Tanabe & Dahl, 2022). Here, we clustered all DsrE-type sequences from the representative genomes of GTDB (release R207) by sequence similarity network (SSN) analysis. In a first approach, the proteins were not filtered for association with dissimilatory sulfur oxidation. Classical TusD/DsrE were clearly distinguishable and only distantly related to the sulfur transferases from the other subclasses (Figure 3c). In a second approach, an SSN was calculated with all DsrE homologs associated with rDsr and/or sHdr systems, excluding the divergent TusD/DsrE proteins (Figure 3d). For DsrE2, DsrE3, and DsrE4 robust clades mirroring the original DsrE groups and subgroups were retrieved (Liu et al., 2014). DsrE3A formed two robust phylogenetic clades, containing archaeal and bacterial sequences, respectively (Figure 3d). DsrE5 proteins present an exception as they do not cluster as a coherent group due to high sequence dissimilarity. While functional predictions for this group are not available, members of the DsrE4 group are proposed to play a role in detoxification of reactive sulfur

species (Liu et al., 2014). As already pointed out, archaeal DsrE3A is an established thiosulfonate carrier whereas DsrE3B and DsrE3C have not been studied on a biochemical level yet. Although a genetic association indicates a function in the sHdr system, the mechanism and specific roles of DsrE3B and DsrE3C have not been described so far.

Once the sulfur transferases could be confidently categorized, their co-occurrence in sHdr-containing organisms was studied using HMSS2 (Tanabe & Dahl, 2023). In addition, they were mapped onto the phylogenetic tree shown in Figure 2. Of all 397 studied assemblies, 387 encode at least one TusA and 302 of the *shdr* clusters are directly linked to *tusA* genes. The *dsrE2* gene is present in 345 (87%) assemblies and in 199 (50.1%) of the *shdr* gene clusters, making it the second most frequently occurring gene. The *dsrE3A* (200), *dsrE3B* (132), and *dsrE3C* (223) genes are less prevalent. However, when these genes are present, 70%, 90%, and 52%, respectively, are located in the immediate vicinity of *shdr* core genes. The rhodanase-encoding gene *rhd442* is present in only three *shdr* gene clusters from the family *Hyphomicrobiae* (Alphaproteobacteria).

The distribution of DsrE-type sulfur transferases appears to relate to the type of sHdr system (Figure 2). Archaea with type I sHdr system particularly often contain *shdr* genes linked with *tusA*, *dsrE3A*, and *dsrE4*. This is different in bacteria with type I sHdr system, where a *tusA/dsrE3C* combination occurs in the same genome at a notably high frequency. Other DsrE-type sulfur transferases may be present but are less abundant. Some members of the Pseudomonadota and Aquificota simultaneously encode DsrE3A and DsrE3B. The highest number of different sulfur transferases is found in genomes from the gammaproteobacterial orders Acidithiobacillales, Acidiferrobacterales, and Ectothiorhodospirillales (here in the genus *Thioalkalivibrio* and in the family Acidihalobacteraceae). These organisms have the genetic potential for DsrE2, DsrE3A, DsrE3B, DsrE3C, and DsrE4. Type II sHdr systems are predominantly associated with TusA and DsrE3A, while DsrE3B and DsrE3C are only very rarely present (Figure 2). Among the type II-containing archaea of the phylum Thermoplasmata, the sulfur transferase DsrE3B is the only transferase present and is genetically associated with the *shdr* cluster.

2.3 | Properties of sHdr associated TusA

The TusA proteins from *Hm. denitrificans* (HdTusA), *Thioalkalivibrio* sp. K90mix (TkTusA), *Ts. sibirica* (TsTusA), and *Aq. aeolicus* (AqTusA), all of which are

encoded in type I *shdr* gene clusters, were selected as model proteins for further analysis. All four proteins contain a highly conserved cysteine within an N-terminal CPXP motif, which is characteristic for the active site of TusA proteins (Figure 4a). Leucine and isoleucine have been described at the X position for TusA proteins involved in sulfur oxidation (Tanabe et al., 2019). A second cysteine is present at equivalent positions in AqTusA, HdTusA and *E. coli* TusA (Figure 4a). This cysteine is not involved in sulfur transfer in *E. coli* (Shi et al., 2010).

Recombinant HdTusA, TkTusA, TsTusA, and AqTusA were purified in the absence of reducing agents. Mass spectrometry verified the masses without initiator methionine for all recombinant TusA proteins (Tables 1 and S2). AqTusA was found to be glutathionylated to a small extent. This is likely a heterologous production artifact because the genes for the enzymes for biosynthesis of glutathione do not occur in the *Aq. aeolicus* genome (Deckert et al., 1998). Upon native PAGE under non-reducing conditions, at least two bands were observed for

all TusAs. In accordance, McTusA has been reported to occur both as monomers and dimers (Liu et al., 2014). Reduction with DTT resulted in the formation of faster migrating bands partially for AqTusA and TkTusA and completely for HdTusA and TsTusA. These bands likely represent monomeric TusA.

To elucidate the capacity of TusA from our four sHdr-containing model sulfur oxidizers for sulfur mobilization from inorganic and organic sulfur compounds, the purified proteins were incubated with 5 mM polysulfide ($^-SS_nS^-$), thiosulfate ($S_2O_3^{2-}$), tetrathionate ($S_4O_6^{2-}$), and oxidized glutathione (GSSG) and analyzed by MALDI-TOF mass spectrometry. All reacted with polysulfide, resulting in mass increases of 32, 64, or 96 Da, corresponding to the addition of one to three sulfur atoms (Tables 1 and S2). After incubation with tetrathionate, mass increases corresponding to addition of one or two sulfur atoms, a thiosulfonate group ($-SSO_3^-$), or $-SSSO_3^-$ were detected. With oxidized glutathione, mass increases of 305 Da were observed for TkTusA, AqTusA, and HdTusA, which corresponds to covalently bound

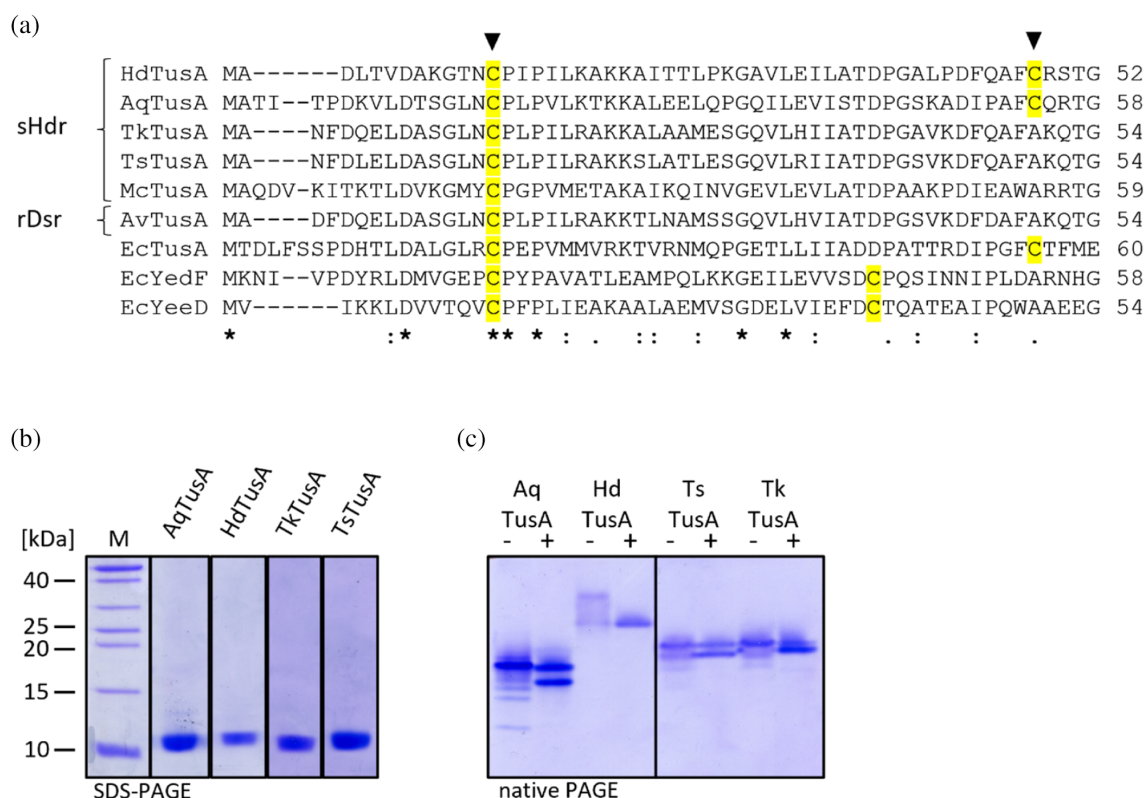


FIGURE 4 (a) Alignment of a portion of TusA and related proteins from sulfur oxidizers and *E. coli*. Ec, *E. coli* (TusA, b3470, YedF, b1930, YeeD, and b2012); Ts, *Ts. sibirica* (ThisiDRAFT_0966, according to JGI IMG); Tk, *Thioalkalivibrio* sp. K90mix (TK90_0631); Av, *Ac. vinosum* (Alvin_2600); Hd, *Hm. denitrificans* (Hden_0698); Aq, *Aq. aeolicus* (Aq_388a); Mc, *Ms. cuprina* (Mcup_0683). Triangles indicate the cysteines that were exchanged to serine in this work. Asterisk, fully conserved residues; colon, conservation between groups of strongly similar properties; dot, conservation between groups of weakly similar properties. (b) 20% SDS-PAGE of recombinant TusAs HdTusA, TkTusA, TsTusA, and AqTusA reduced with DTT. (c) 20% native PAGE of 3.5 μ g recombinant TusAs HdTusA, TkTusA, and TsTusA and AqTusA as purified (-) and reduced with 5 mM DTT (+).

TABLE 1 Sulfur loading of native and variant TusA and DsrE3 proteins.

Protein	Expected masses [Da]	Detected masses [Da]	Modification
HdTusA + polysulfide	9149	9149	-
		9180 ($\Delta 31$)	-S
		9208 ($\Delta 60$)	-S ₂
		9238 ($\Delta 90$)	-S ₃
HdTusA Cys ¹³ Ser + polysulfide	9135	9135	-
HdTusA + S ₄ O ₆ ²⁻	9149	9150	-
		9148 ($\Delta 34$)	-S
		9212 ($\Delta 62$)	-S ₂
		9262 ($\Delta 112$)	-S-SO ₃
		9296 ($\Delta 146$)	-S ₂ -SO ₃
AqTusA + polysulfide	9610	9612	-
		9643 ($\Delta 31$)	-S
AqTusA Cys ¹⁷ Ser + polysulfide	9595	9595	-
AqTusA Cys ⁵⁴ Ser + polysulfide	9595	9596	-
		9627 ($\Delta 31$)	-S
AqTusA + S ₄ O ₆ ²⁻	9610	9610	-
		9642 ($\Delta 32$)	-S
		9724 ($\Delta 114$)	-S-SO ₃
		9755 ($\Delta 145$)	-S ₂ -SO ₃
AqTusA Cys ¹⁷ Ser + S ₄ O ₆ ²⁻	9595	9595	-
AqTusA Cys ⁵⁴ Ser + S ₄ O ₆ ²⁻	9595	9597	-
		9630 ($\Delta 33$)	-S
		9710 ($\Delta 113$)	-S-SO ₃
HdDsrE3C + polysulfide	15,520	15,524	-
		15,561 ($\Delta 38$)	-S
		15,588 ($\Delta 64$)	-S ₂
		15,621 ($\Delta 98$)	-S ₃
HdDsrE3C Cys ⁸³ Ser + polysulfide	15,504	15,503	-
		15,535 ($\Delta 32$)	-S
HdDsrE3C Cys ⁸⁴ Ser + polysulfide	15,504	15,503	-
HdDsrE3C + S ₄ O ₆ ²⁻	15,520	15,517	-
		15,610 ($\Delta 93$)	-S ₃
		15,629 ($\Delta 112$)	-S-SO ₃ ⁻
		15,658 ($\Delta 141$)	-S ₂ -SO ₃ ⁻
HdDsrE3C + GSSG	15,520	15,518	-
		15,824 ($\Delta 305$)	-SG
TkDsrE3B + polysulfide	17,201	17,205	-
		17,236 ($\Delta 31$)	-S
		17,320 ($\Delta 115$)	-S-SO ₃ ⁻
TsDsrE3B + polysulfide	16,619	16,619	-
		16,653 ($\Delta 34$)	-S
		16,683 ($\Delta 64$)	-S ₂
		16,736 ($\Delta 117$)	-S-SO ₃ ⁻

Note: Numbers in parentheses represent mass increases. -, no modification. Further information is available in Table S2.

glutathione. The mobilization abilities for the bacterial TusAs AqTusA, TkTusA, TsTusA, and HdTusA differed from those reported for archaeal TusA, which only mobilized thiosulfonate from tetrathionate but not sulfane sulfur from polysulfide. Like McTusA (Liu et al., 2014), none of the studied bacterial TusA proteins were modified by thiosulfate.

To identify the sulfur-binding cysteine with certainty, the cysteine of the CPXP motif was replaced by serine in both, HdTusA and AqTusA, as was the C-terminal partially conserved cysteine of AqTusA. No additional peaks were observed when AqTusA Cys¹⁷Ser or HdTusA-Cys¹³Ser were incubated with sulfur compounds. AqTusA Cys⁵⁴Ser reacted with polysulfide and tetrathionate just as wild type AqTusA. The cysteine of the CPXP motif was thus confirmed as the sulfur-binding cysteine.

2.4 | Properties of sHdr-associated Rhd442

The ability of rDsr associated rhodanese Rhd_2599 to transfer sulfur to the TusA protein encoded next to its gene has already been demonstrated for *Ac. vinosum* (Stockdreher et al., 2014) and there is no reason to doubt that closely related enzymes from other sulfur oxidizers (Figure 3b) exert the same function. All these proteins are single domain rhodanases featuring a classical CRXGC[R/T] motif (Bordo & Bork, 2002). On the other hand, information about the putative single domain rhodanese Rhd442 encoded in the vicinity of hyphomicrobial type I *shdr* clusters (Figure 1) is limited. Rhd442 has been described as a domain fused to sulfide: quinone oxidoreductase (SQR), for example, in *Cupriavidus pinatubonensis* and that domain (CpRhd442) was shown to have rhodanese activity (Xin et al., 2016). The activity depended on the cysteine residue in the CRXGXR motif that the domain shares with classical rhodanese (Bordo & Bork, 2002; Ran et al., 2022). A sequence reminiscent of that motif is also present in sHdr-associated Rhd442 (Figure 5a). The AlphaFold models of HdRhd442 and CpRhd442 are similar (Figure 5b) and there is also high consistency with the crystal structure of a non-classical phosphatase from *Neisseria meningitidis* (PDB 2F46 (Krishna et al., 2007)) (Figure 5c). Recombinant HdRhd442 catalyzed sulfur transfer from thiosulfate to cyanide with a maximum specific activity of 360 mU/mg in the assay described by Ray et al. (2000). Furthermore, the protein proved able to mobilize sulfur from polysulfide as shown by characteristic mass increases (Figure 5d,e).

2.5 | Function and properties of sHdr-associated DsrE proteins

Analysis of recombinant DsrE3B from *Thioalkalivibrio* sp. K90mix and DsrE3C from *Hm. denitrificans* by gel permeation chromatography showed two peaks, one corresponding to the monomeric size and the other corresponding to a trimer (Figure 6a). Applying HdDsrE3C to native PAGE revealed a ladder of bands corresponding to higher oligomers (Figure 6b). Reduction of DsrE3C with 5 mM DTT resulted in a shift of the band pattern towards lower oligomers in relation to the non-reduced protein (Figure 6b). The structure of the trimeric complex was modeled by AlphaFold (Figure 6c). Notably, the attempt to predict a hexamer for HdDsrE3C resulted in a complex which oligomerized by protein-protein interaction at the surface of only two subunits of each trimer, leaving two subunits for further docking with other units.

Recombinant DsrE3C and DsrE3B had masses corresponding to the polypeptides without the N-terminal starting methionine. In all cases of DsrE3B, modified species were detected that correspond to glycosylated derivatives (+178 Da) (Table 1, Figures S3 and 7b). This is due to the well documented addition of glucose to the His-tag of the recombinant proteins produced in *E. coli* (Geoghegan et al., 1999). Sulfur mobilization assays showed reaction of HdDsrE3C with polysulfide, tetrathionate, and GSSG but not with thiosulfate. The DsrE3B proteins were persulfidated upon incubation with polysulfide. Oxidized species also occurred, probably due to the presence of oxygen. DsrE3C from *Hm. denitrificans* has an additional cysteine (Cys⁸³) residing right next to the conserved cysteine (Cys⁸⁴). To unambiguously identify the active site sulfur binding cysteine, both cysteines of HdDsrE3C were replaced with serine. While the Cys⁸³Ser mutation did not significantly affect the sulfur binding properties of HdDsrE3C, the HdDsrE3C Cys⁸⁴Ser variant was no longer persulfidated by polysulfide. In conclusion, Cys⁸⁴ of HdDsrE3C was identified as the sulfur-binding cysteine.

Hm. denitrificans is accessible to genetic manipulation and indeed, the analysis of a mutant strain lacking *dsrE3C* provided important information. The deletion was established in the *Hm. denitrificans* Δ *tsdA* reference strain (Koch & Dahl, 2018; Li, Koch, et al., 2023) that completely oxidizes thiosulfate via the sHdr-pathway (Figures 6d and S1). Compared with the reference strain, *Hm. denitrificans* Δ *tsdA* Δ *dsrE3C* oxidized thiosulfate with a significantly decreased specific oxidation rate (Figure 6d). Thus, DsrE3C is crucial for the functionality of the sHdr system. In addition, the importance of the conserved Cys⁸⁴ and the non-conserved Cys⁸³ of HdDsrE3C was studied in vivo by replacing them with

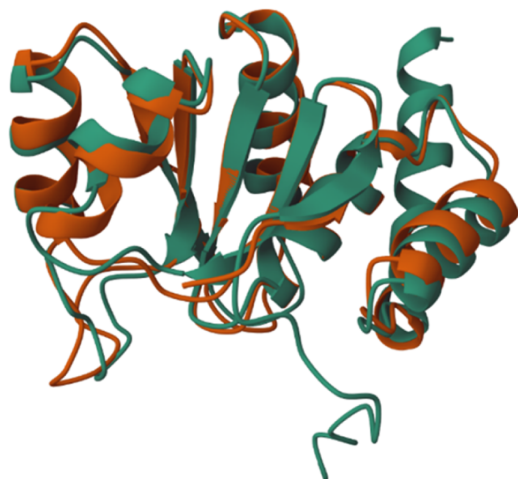
(a)

```

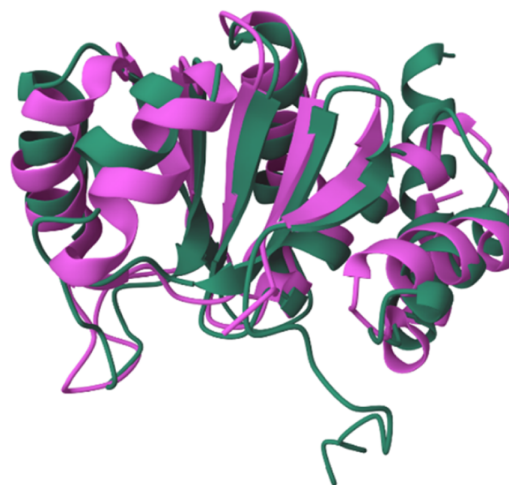
HdRhd442    IINNQPETDEDLLMTPNEVATEAESVGLSYVHIPVEGRNPLEKDVRRFHDALTSLPPPIFAFCKTGGRSASLWAMASVADLDTETLISRCHH 43-135
HsRhd442    IINNQPSDDGLMLGSEVAEAGAVGLSYLHIPVEGRNPLEKDVRRFGHALETLPGPPIFAYCRTGGRSASLWAMASVHLNDTEALIACRQ 43-135
AWRhd442    LNNRPDGEKDSPMTSAEAEAVASSLGLAYMHIPVEGRNPLEKDVRAFAQALKALPQPIYAFCQSGGRSAALWALASVTEATTEALVTTCAR 56-148
CsRhd442SQR LICNRPDGEKDPQPGFQEIERKAFALGLQVHYLPVESGKVSDEQAQAFGQLDLSLKPVLAYCRTGTRSATLWALSQSARRPLPDIIERAAA 31-123
CpRhd442SQR LICNRPDGEKDPQPNFQEIERKASALGLQAHYLPVESGKVSDEQAQAFGQLDLSLKPVLAYCRTGTRSATLWALSQSVIRPLPDIIERAAA 31-123
PaRhd442SQR VICNRPDGEKSDQPLFAEIKRAADAVGIEAHYLPAESGKVTDEQGIAFGELLETLPKPVLAYCRSGMRSTTMWALSQAGQHDLPHIVESAKK 31-123
      :* *:* :      *      * :*: :*: .|. :  : :      * . * :** * :*:*:* **::**:: :      : :

```

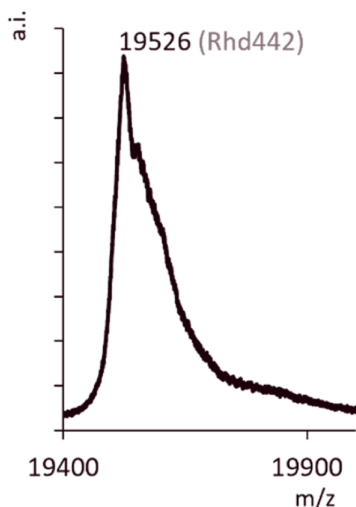
(b)



(c)



(d)



(e)

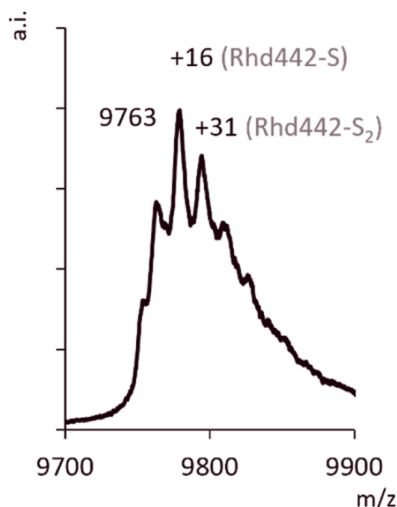


FIGURE 5 (a) Alignment of single domain Rhd442 from *Hm. denitrificans* (Hd), *Hyphomicrobium* sp018242215 (Hs), and AWTP1-13-sp008933705 (AW) with Rhd442 domains fused to sulfide: quinone oxidoreductase (SQR) from *Cupriavidus* sp. amp6 (Cs), *Cupriavidus pinatubonensis* (Cp), *Pseudomonas veronii* (Pa) (Xin et al., 2016). Partially and fully conserved cysteines are highlighted in yellow. Sequences conforming to the rhodanese active site sequence logos (Ran et al., 2022) are shaded in gray. Asterisk, fully conserved residues; colon, conservation between groups of strongly similar properties; dot, conservation between groups of weakly similar properties. (b) HdRhd442 AlphaFold structure (green) overlaid with Rhd442 domain of *Cv. pinatubonensis* SQR (brown) and (c) non-classical phosphatase from *Ns. meningitidis* (PDB 2F46, purple). (d) Mass spectrum of recombinant HdRhd442 as isolated. (e) HdRhd442 mass spectrum after incubation with 0.5 mM polysulfide. Note that a distinguishable signal for Rhd442 and its persulfidated species was only observable for the double ionized protein.

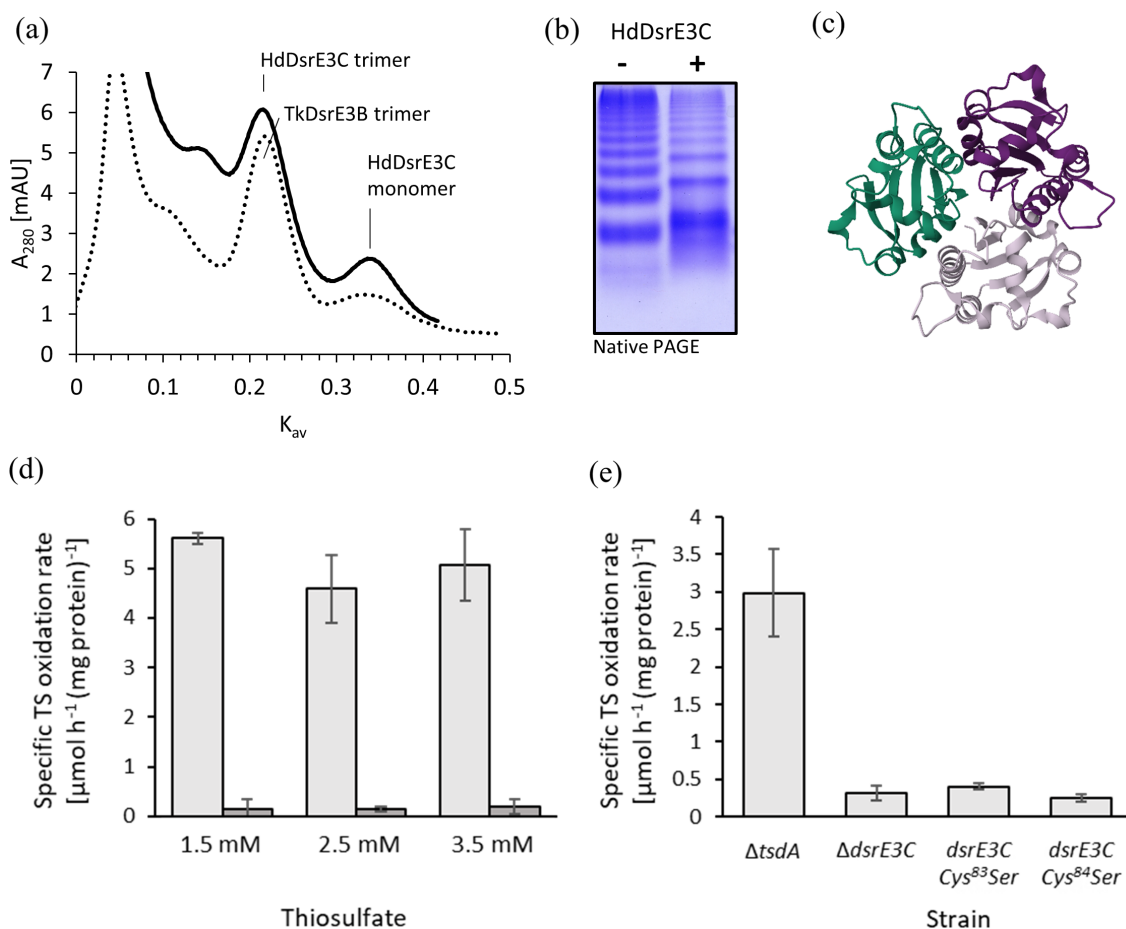


FIGURE 6 Function and properties of DsrE3B and DsrE3C proteins. (a) Gel permeation chromatography of HdDsrE3C and TkDsrE3B on Hiloal 16/60 Superdex 75. (b) Native-PAGE of 3.5 μg HdDsrE3C as purified (–) and reduced with 5 mM DTT (+). (c) AlphaFold model of the HdDsrE3C trimer. (d) Specific thiosulfate (TS) oxidation rates for *Hm. denitrificans* ΔtsdA (light gray columns) and *Hm. denitrificans* ΔtsdA ΔdsrE3C (dark gray columns) at the indicated initial thiosulfate concentrations. The corresponding growth curves are provided in Figure S1. Precultures contained 2 mM thiosulfate. (e) Specific thiosulfate oxidation rates of *Hm. denitrificans* ΔtsdA compared to a strain lacking the complete *dsrE3C* gene and two strains carrying *dsrE3C* genes encoding the indicating cysteine to serine exchanges grown with 2.5 mM thiosulfate. Note that specific thiosulfate oxidation rates are not fully comparable to the experiments shown in (d) because the growth experiments shown here were performed in a plate reader.

serine. Both exchanges resulted in significantly decreased specific thiosulfate oxidation rates compared to the reference strain (Figure 6e). We conclude that, although it is not involved in sulfur binding, Cys⁸³ is important for DsrE3C function in vivo.

2.6 | Interactions of sHdr-associated sulfur transferases

The persulfidated DsrE3 proteins from our proteobacterial model organisms *Ts. sibirica*, *Thioalkalivibrio* sp. K90 and *Hm. denitrificans* were used as donors for the TusA proteins from the same organism, resulting in sulfur transfer as shown by mass spectrometry (Figures 7a, S2a, S3a, and Table S3). Quantitative comparison of MALDI-

TOF MS data from different samples is difficult and prone to errors (Szajli et al., 2008), however, we can confidently state that a significant proportion of the detected TusA molecules received sulfur from TsDsrE3B. In contrast, in the opposite direction, when TusA acted as a donor for the DsrE3 proteins, only a minority of the DsrE3 molecules detected by MALDI-TOF MS were persulfidated, if any sulfur was added at all (Figures 7b, S2b, S3b, and Table S3). These in vitro results point at DsrE3 proteins transferring sulfur to TusA in vivo, whereas the opposite direction is unfavorable. Neither recombinant HdTusA-Cys¹³Ser nor HdDsrE3C-Cys⁸⁴Ser accepted sulfur from the native persulfidated donor proteins, whereas HdDsrE3C-Cys⁸³Ser accepted sulfur from persulfidated HdTusA (Table S3). The Cys⁸³Ser mutation did not significantly affect the sulfur transfer properties of HdDsrE3C,

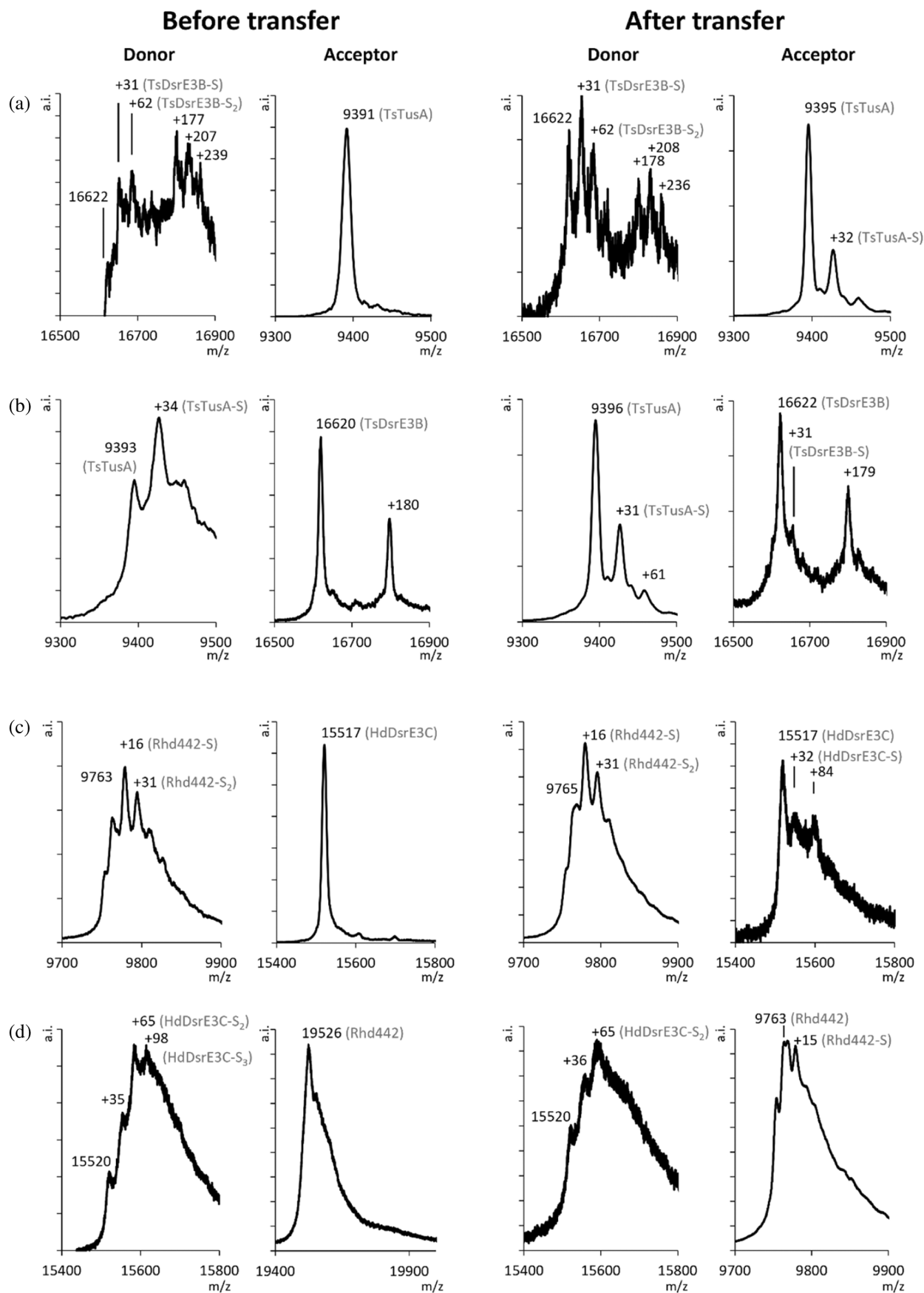


FIGURE 7 Legend on next page.

while the HdDsrE3C Cys⁸⁴Ser variant was persulfidated neither by polysulfide (see above) nor by HdTusA.

Persulfidated HdRhd442 was tested as sulfur donor for HdTusA and HdDsrE3C. Sulfane sulfur from HdDsrE3C was efficiently transferred to HdRhd442 (Figure 7c). Transfer from HdDsrE3C to HdRhd442 was also efficient (Figure 7d). With HdTusA as the acceptor molecule for HdRhd442, the transfer was inefficient as the intensity of the signal corresponding to the sulfidated species was low compared to the signal for the unmodified protein (Figure S4a). Upon transfer in the opposite direction, the majority of Rhd442 detected by MALDI-TOF MS was persulfidated (Figure S4b).

2.7 | TusA and DsrE3C, DsrE3B and DsrE2 from *Aq. aeolicus* interact

Aq. aeolicus is an excellent model organism for identifying interactions between sHdr-associated sulfur transferases and other proteins. Membrane fractions, cell extracts, and partially purified proteins from this hyperthermophile have repeatedly served as the basis for cross-linking, co-purification and co-migration approaches, which have enabled the identification of physiological protein partners (Aussignargues et al., 2012; Boughanemi et al., 2016; Prioretti et al., 2023). Here, we incubated pure recombinant His-tagged AqTusA with *Aq. aeolicus* soluble extracts, prepared from cells that had been grown in the presence of thiosulfate and hydrogen (Boughanemi et al., 2016) at room temperature as specified in Section 5. In all these experiments, recombinant AqTusA showed a mass gain of 32 Da, indicating a bound sulfane sulfur after re-purification from the cell extract. This may be attributed to a transfer of sulfur originating from the cell extract since the heterologously produced AqTusA did not exhibit such masses after purification (Tables 1 and S2).

In a first approach, all proteins that were co-purified with recombinant AqTusA from *Aq. aeolicus* cell extract were analyzed. Cell extract and recombinant AqTusA

were incubated at room temperature for 30 min, followed by the re-purification of AqTusA from the extract by affinity chromatography and identification of all co-purified proteins by mass spectrometry. Cell extract without the addition of His-tagged TusA served as negative control and was similarly applied to affinity chromatography and mass spectrometry. The comparison of the purified proteins from both samples revealed 253 proteins that were exclusively present after re-purification of the recombinant AqTusA. Among them, AqDsrE3C (aq_390) was identified with one of the highest scores (Table S4). AqDsrE2A (aq_389) also eluted specifically in the

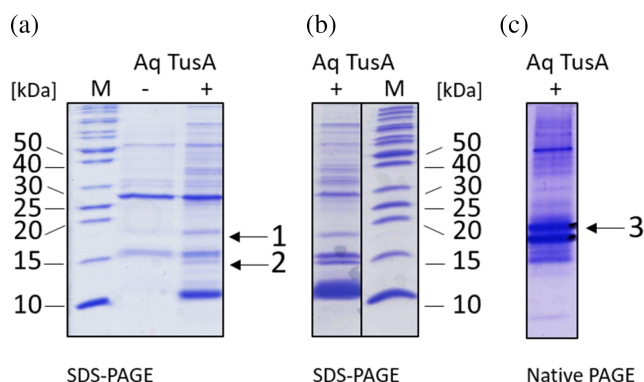


FIGURE 8 Re-purification experiments of recombinant AqTusA after incubation with *Aq. aeolicus* soluble extract in different conditions. (a) Proteins eluted after 30 min incubation of AqTusA with *Aq. aeolicus* soluble extract and separated on a 18% SDS-PAGE. ‘-’ corresponds to the proteins retained in the control experiment lacking AqTusA (extract only, negative control). ‘+’ corresponds to retained proteins after incubation of soluble cell extract with recombinant AqTusA. Equal volumes of elution fractions, corresponding to 2 and 10 μ g of total protein, were loaded into the lanes. Proteins in bands 1 and 2 were analyzed by mass spectrometry (Table S5). (b) Proteins (6 μ g) eluted after 10 min incubation of AqTusA with *Aq. aeolicus* soluble extract and separated on a 18% SDS-PAGE. (c) Proteins (6 μ g) eluted after 10 min incubation of AqTusA with *Aq. aeolicus* soluble extract and separated on a 15% native PAGE. Proteins in band 3 were analyzed by mass spectrometry (Table S6). Molecular weight markers (kDa) for the SDS gels are shown in lanes ‘M’.

FIGURE 7 Sulfur transfer between TusA, DsrE3 proteins, and Rhd442. Sulfur transfer reaction between TusA and DsrE3B from *Ts. sibirica* and between Rhd442 and DsrE3C from *Hm. denitrificans* are shown as examples. The full set of experiments is available as Figures S2, S3, and S4. (a) Left panels: TsDsrE3B as persulfidated donor after treatment with polysulfide and unmodified reduced TsTusA as acceptor; right panels: DsrE3B (donor) and TusA (acceptor) after the transfer reaction. The TsDsrE3B species exhibiting additional 178 Da are due to glucosylation of the His-Tagged protein (Geoghegan et al., 1999). (b) Left panels: TsTusA as persulfidated donor after treatment with polysulfide and unmodified reduced TsDsrE3B as acceptor; right panels: TsTusA and TsDsrE3B after the transfer reaction. (c) Left panels: HdRhd442 as persulfidated donor after treatment with polysulfide and unmodified reduced HdDsrE3C as acceptor. Right panels: HdRhd442 (donor) and HdDsrE3C (acceptor) after the transfer reaction. (d) Left panels: HdDsrE3C as persulfidated donor after treatment with polysulfide and unmodified reduced HdRhd442 as acceptor. Right panels: HdDsrE3C (donor) and HdRhd442 (acceptor) after the transfer reaction. Note that the spectrum on the far right shows the doubly charged ion.

presence of TusA but was identified with lower score and peptide number. The sHdrB1, sHdrB2, and sHdrC1 subunits of the sHdr complex were also captured in this experiment (Table S4). The polypeptides sHdrA and sHdrC2 as well as LbpA2 (aq_402) were identified, but were also present in the control sample (Table S4). Of the remaining proteins, 85 were associated with protein biosynthesis and degradation, and 24 were related to known or proposed functions of TusA other than sulfur oxidation, such as tRNA modification, molybdopterin cofactor biosynthesis and regulation (Dahl et al., 2013; Ikeuchi et al., 2006; Li, Törkel, et al., 2023). To gain further insight into the interaction partners of AqTusA, the re-purified samples were applied to SDS-PAGE (Figure 8a). Bands that were present exclusively in the TusA-containing sample were analyzed by mass spectrometry. In one of these bands, AqDsrE2A (aq_389) was found together with LbpA3 (aq_1657), a putative thiol peroxidase (aq_488), and 14 additional proteins (Figure 8a, band 1, Table S5). AqDsrE3C and AqLbpA2 were unambiguously detected by mass spectrometry in another band that also contained AqDsrE3B (Aq_401) and 25 other proteins, the majority of which were either uncharacterized proteins, ribosomal proteins or chaperones (Figure 8a, band 2, Table S5).

In the next set of experiments, we increased sensitivity by reducing the incubation time of recombinant AqTusA with cell extract to 10 min. After re-purification and SDS-PAGE, the sample showed a similar band pattern as that of the previous experiment (Figure 8b). To more specifically analyze the interaction partners of AqTusA, we then tested co-migration in native PAGE (Figure 8c). Analysis of a prominent band revealed the presence of TusA together with AqDsrE3C (Aq_390) and AqLbpA2 (Aq_402) alongside 12 other proteins (Figure 8c, band 3, Table S6).

3 | DISCUSSION

When bound to a large molecule like a protein, persulfidic sulfane sulfur can be handled with high specificity (Kessler, 2006). The sulfur transferases examined in this work perfectly illustrate this concept. Several independent lines of evidence have been combined to strongly suggest an important function for TusA- and DsrE3-type sulfur transferases in sulfur-oxidizing prokaryotes utilizing the sHdr pathway. First, the respective genes not only frequently occur in this physiological group (Figure 2), but in the majority of cases they co-localize with *shdr* genes (Figures 1 and 2), similar to what has been observed for the second well-established cytoplasmic oxidation pathway in sulfur-dependent lithotrophs, rDsr (Stockdreher et al., 2014). Rhodanese Rhd442 is present

in only a small number of sulfur oxidizers and therefore appears to be of minor importance. Second, deletion of the gene for DsrE3C from *Hm. denitrificans* resulted in a thiosulfate oxidation-negative phenotype, emphasizing the importance of the sulfur transferase. Third, the studied proteins all demonstrated the ability to bind sulfur upon incubation with inorganic polysulfide and transfer it to interaction partners, therefore acting as components of a sulfur trafficking cascade or network.

The investigated DsrE3B and DsrE3C proteins from bacteria were characterized as stable homotrimers in solution that have a tendency to assemble into higher oligomers, particularly hexamers. This is consistent with the available data on DsrE3A proteins from archaea. The homotrimeric form of the protein is observed in solution for the *Ms. cuprina* protein, and the *Saccharolobus solfataricus* (SSO1125) protein crystallizes as a trimer (PDB ID 3MC3). The DsrE2B sulfur transferases from the same archaea also form homotrimers (PDB ID 2QS7) (Liu et al., 2014). In sulfur oxidizers utilizing the rDsr pathway, the heterohexameric DsrE₂F₂H₂ complex plays a vital role in the sulfur relay system, which supplies the oxidizing enzyme rDsrAB. The subunits are arranged in two stacked DsrEFH rings, each resembling the trimeric rings observed in DsrE3A crystals (PDB ID 3MC3) and DsrE3C AlphaFold models (Figure 6c). DsrE, DsrF, and DsrH are related to each other (Dahl et al., 2008). In summary, the formation of trimers is a general and common property of DsrE and DsrE3-type proteins, that has been conserved throughout evolution. It is probable, that the three distinct subunits in DsrEFH have evolved due to gene duplications and specialization of ancestral DsrE-type proteins. In fact, from an evolutionary perspective, the DsrE3 proteins are older than the DsrE in DsrEFH (Neukirchen et al., 2023). Filamentation has not been reported for the DsrEFH complex nor for any other DsrE-type; it is a novel characteristic of DsrE3C from *Hm. denitrificans*. As previously stated, all DsrE-like proteins possess a single conserved cysteine residue (Cys⁸⁴ in HdDsrE3C). The importance of the equivalent cysteine for sulfur binding and transfer has so far only been shown in vitro for the *Ms. cuprina* protein DsrE3A and both in vivo and in vitro for the distantly related DsrE from the *A. vinosum* DsrEFH complex. Here, we prove the crucial role of this residue through in vivo and in vitro studies on DsrE3C from *Hm. denitrificans*. Furthermore, we show that the adjacent Cys⁸³ is important for DsrE3C function in vivo, even though it does not participate in sulfur binding.

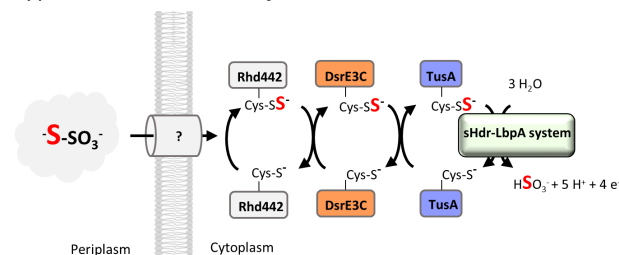
Just like archaeal McDsrE3A (Liu et al., 2014), all DsrE3B, DsrE3C, and TusA proteins from bacteria that were examined in this study displayed reaction with tetrathionate in vitro. Indeed, *Ms. cuprina* utilizes

tetrathionate as an electron donor (Liu et al., 2011, 2014). However, it is impossible that thiosulfonates derived from tetrathionate are the physiologically relevant form of sulfur processed in the cytoplasm of the bacteria studied here. Neither *Hm. denitrificans* (Koch & Dahl, 2018) nor *Thioalkalivibrio* sp. K90mix (Muyzer et al., 2011), *Aq. aeolicus* (Boughanemi et al., 2020) or *Ts. sibirica* (Bryantseva et al., 1999) can metabolize tetrathionate. If we seek a type of sulfur that every organism studied can use as a cytoplasmic sulfur currency, then only polysulfide or sulfane sulfur is left, as *Ts. sibirica* cannot oxidize thiosulfate either (Figure 9). In addition, HdTusA and HdDsrE3C are unable to mobilize sulfane sulfur from thiosulfate in vitro.

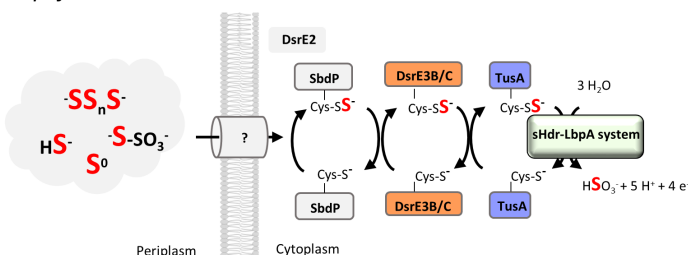
In dissimilatory sulfur oxidizers, the oxidation of sulfide and thiosulfate is always initiated outside of the cytoplasm (Dahl, 2015; Dahl, 2020). In many cases, sulfane sulfur is then imported into the cytoplasm where it is further oxidized (Figure 9). It is not yet clear how this import is accomplished. *Hm. denitrificans* possesses two candidate transporters (SoxT1A and SoxT1B, Figure 1) encoded in close proximity to the genes encoding Sox proteins that are involved in the initial steps of thiosulfate oxidation and the genes for the cytoplasmic sHdr system (Li, Koch, et al., 2023; Li, Törkel, et al., 2023). However, evidence supporting the proposed sulfur

transport has yet to be presented. Related transporters are not encoded in *Aq. aeolicus* and *Ts. sibirica* such that they cannot be of general importance. Rhodanese-like sulfur transferases including Rhd442, with its comparatively narrow distribution, are potential primary sulfur acceptors and distributors in the cytoplasm. They occur in all examined organisms (Figures 1, 2, and 9) and have well established sulfur transfer activity. HdRhd442 was shown here to interact with HdDsrE3C. This protein, in turn, was established as an indispensable component of the sulfur-handling cascade that feeds the type I sHdr system of *Hm. denitrificans*. In vitro, both HdDsrE3C and the DsrE3B proteins from gammaproteobacterial model organisms shuttle sulfane sulfur to TusA (Figures 7 and 9). Efficient sulfur transfer to TusA from the same organism was observed with HdDsrE3C, TkDsrE3B, and TsDsrE3B. With DsrE proteins as donors, up to half of the TusA proteins that were detected by mass spectrometry were persulfidated after the transfer. In the opposite direction, transfer to HdDsrE3C was never detectable, while negligible amounts of TkDsrE3B and TsDsrE3B were modified. Unidirectional transfer has also been observed for DsrE3A and TusA from *Ms. cuprina*, where a thiosulfonate group is moved from DsrE3A to TusA but not vice versa (Table S7) (Liu et al., 2014). In the absence of a DsrE3C homolog, as in *Thioalkalivibrio*

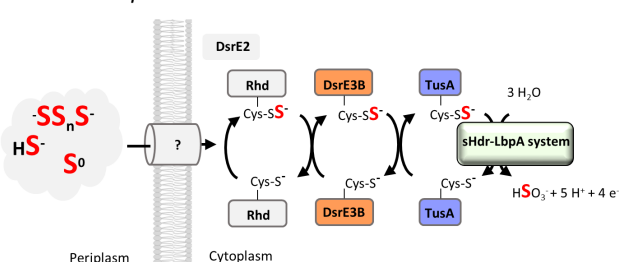
Hyphomicrobium denitrificans



Aquifex aeolicus



Thiorhodospira sibirica



Thioalkalivibrio sp. K90mix

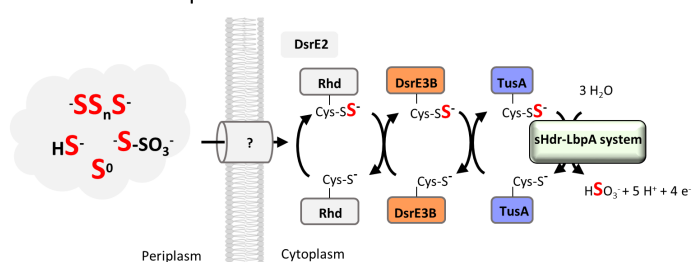


FIGURE 9 Sulfur relay systems in the four bacterial model organisms studied in this work. *Hm. denitrificans* oxidizes thiosulfate and dimethyl sulfide. Thiosulfate is an intermediate of DMS oxidation (Cao et al., 2018; Koch & Dahl, 2018). *Aq. aeolicus* (Deckert et al., 1998) and *Thioalkalivibrio* sp. K90mix (Muyzer et al., 2011) metabolize a wide range of inorganic sulfur substrates including thiosulfate, whereas *Ts. sibirica* is unable to oxidize thiosulfate (Bryantseva et al., 1999). It was originally predicted that DsrE2A from *Aq. aeolicus* (Aq_389) is bound to the membrane via two transmembrane segments. However, recent deep-learning based programs like DeepTMHMM (Hallgren et al., 2022) challenge this view not only for the *Aquifex* protein but also for the corresponding enzymes found in *Ts. sibirica* and *Thioalkalivibrio* sp. K90mix.

sp. K90mix, the sulfur transferase DsrE3B may functionally substitute for DsrE3C. It is very important to note that each sulfur transferase may interact with multiple partners as illustrated by TusA from *Aq. aeolicus* which was purified along with three DsrE, two AqLbpA and several sHdr proteins. This finding is particularly significant as it establishes a direct link between sulfur transferases and the sHdr–LbpA complex where sulfane sulfur is oxidized to sulfite (Cao et al., 2018; Ernst et al., 2021; Koch & Dahl, 2018).

4 | CONCLUSIONS

We conclude that cytoplasmic sHdr systems for sulfane sulfur oxidation are always accompanied by sets of sulfur transferases. The exact composition of these sets may vary (Figure 9). In vivo, a strict unidirectional transfer of sulfur between the components is unlikely. Rather, it can be assumed that a network of sulfur-binding proteins exists, each with a pool of bound sulfur. Sulfur flux can be shifted in one direction or the other depending on the metabolic requirements. A single pair of sulfur-binding proteins with a preferred transfer direction, such as a DsrE3-type protein towards TusA, may well be sufficient to push sulfur into the sink where it is further metabolized or needed. Multiple possible interactions are most easily exemplified for the TusA protein. In organisms such as *Hm. denitrificans*, which differ from *E. coli* by containing just one *tusA* gene, the same protein must likely fulfill a variety of functions, including providing substrate for sulfur oxidation, and supplying sulfur for tRNA thiolation and biosynthesis of cofactors and Fe/S clusters.

5 | MATERIALS AND METHODS

5.1 | Bacterial strains, plasmids, primers, and growth conditions

Table S8 lists the bacterial strains, and plasmids that were used for this study. *Escherichia coli* strains were grown on complex lysogeny broth (LB) medium (Bertani, 2004) under aerobic conditions at 37°C unless otherwise indicated. *E. coli* 10β was used for molecular cloning. *E. coli* BL21 (DE3) was used for recombinant protein production. *Hm. denitrificans* strains were cultivated in minimal media kept at pH 7.2 with 24.4 mM methanol and 100 mM 3-(*N*-morpholino) propanesulfonic acid (MOPS) buffer as described before (Koch & Dahl, 2018; Li, Koch, et al., 2023). Thiosulfate was added as needed. Antibiotics for *E. coli* and *Hm.*

denitrificans were used at the following concentrations (in μg/mL): ampicillin, 100; kanamycin, 50; streptomycin, 200; and chloramphenicol, 25.

5.2 | Recombinant DNA techniques

Standard techniques for DNA manipulation and cloning were used unless otherwise indicated (Ausubel et al., 1997). Restriction enzymes, T4 ligase and Q5 polymerase were obtained from New England Biolabs (Ipswich, UK) and used according to the manufacturer's instructions. Oligonucleotides for cloning were obtained from Eurofins MWG (Ebersberg, Germany). Plasmid DNA from *E. coli* was purified using the GenJET Plasmid Miniprep Kit (Thermo Scientific, Waltham, USA). Chromosomal DNA from *Hm. denitrificans*, *Ts. sibirica*, and *Thioalkalivibrio* strains was prepared using the Simplex easy DNA kit (GEN-IAL GmbH, Troisdorf, Germany). Total DNA from 20 mg of *Aq. aeolicus* cells was extracted using the phenol–chloroform extraction method. Cells were resuspended in 150 μL of TEN buffer (10 mM Tris pH 8, 150 mM NaCl, and 10 mM EDTA) and 300 μL of SDS-EB (100 mM Tris pH 8, 400 mM NaCl, 40 mM EDTA, and 2% SDS). 2 μL of RNase A solution (4 mg/mL) (Promega) were added before incubation at 37°C for 15 min. 350 μL phenol/chloroform–isoamylalcohol (25:24:1 mixture, Biosolve) were added and the mixture was vortexed for 30 s and spun for 3 min at 14,000 × g. The upper phase was transferred to a new tube with 300 μL of chloroform–isoamylalcohol, vortexed and spun again. The upper phase was then incubated with 600 μL isopropanol for 30 min at –25°C and spun at 4°C for 30 min. The DNA pellet was washed with 70% ethanol, left to air dry and dissolved in 100 μL H₂O for 30 min at 65°C. 1 μL was used for 25 μL PCR reaction.

5.3 | Construction of *Hm. denitrificans* mutant strains

For markerless deletion of the *Hm. denitrificans* *dsrE3C* (Hden_0688) gene by splicing overlap extension (SOE) (Horton, 1995), PCR fragments were constructed using the primers Hden0688_Up_Fw, Hden0688_Up_Rev, Hden0688_Down_Fw, Hden0688_Down_Rev (Table S1). The resulting 2.08 kb SOE PCR fragment was cloned into the *Xba*I and *Pst*I sites of pK18mobsacBC-Tc. The final construct pK18mobsacB_Tc_Δ*dsrE3C* was electroporated into *H. denitrificans* Δ*tsdA* and transformants were selected using previously published procedures (Cao et al., 2018; Koch & Dahl, 2018). Single crossover recombinants were Cm^r and Tc^r. Double crossover

recombinants were Tc^s and survived in the presence of sucrose due to loss of both, the vector-encoded levansucrase (SacB) and the tetracycline resistance gene. For chromosomal integration of the genes encoding DsrE3C Cys⁸³Ser and DsrE3C Cys⁸⁴Ser, the modified genes and upstream as well as downstream sequences were amplified by SOE PCR using primers Hden0688_Up_Fw, Hden0688_Down_Rev, Hden0688_C83S_Fw, Hden0688_C83S_Rev, and Hden0688_Up_Fw, Hden0688_Down_Rev, Hden0688_C84S_Fw, Hden0688_C84S_Rev (Table S1), respectively. The final plasmids pk18*mobsacB*-Tc-dsrE3C-C83S and pk18*mobsacB*-Tc-dsrE3C-C84S were transferred into *Hm. denitrificans* Δ *tsdA* Δ *dsrE3C* and double crossover recombinants were selected as described previously (Koch & Dahl, 2018). The genotypes of the *Hm. denitrificans* mutant strains generated in this study were confirmed by PCR.

5.4 | Characterization of phenotypes and quantification of sulfur compounds

Growth experiments with *Hm. denitrificans* were run in Erlenmeyer flasks with media containing 24.4 mM methanol and varying concentrations of thiosulfate as necessary (Li, Koch, et al., 2023). Thiosulfate and sulfite concentrations and biomass content were determined by previously described methods (Dahl, 1996; Li, Koch, et al., 2023). All growth experiments were repeated three to five times. Representative experiments with two biological replicates for each strain are shown. All quantifications are based on at least three technical replicates. Alternatively, growth experiments were run in 48-well microtiter plates. Plates were continuously shaken at 200 rpm and growth was followed by measuring optical density at 600 nm every 5 min using an Infinite 200Pro (Tecan, Crailsheim, Germany) plate reader. Samples for thiosulfate determination were taken as previously described (Li, Koch, et al., 2023).

5.5 | Cloning, site-directed mutagenesis, overproduction, purification, and size exclusion chromatography of recombinant proteins

The 378-bp *dsrE3C* gene was amplified from *Hm. denitrificans* genomic DNA with the primers Hden0688 (*dsrE3C*)_NdeI_fw and Hden0688 (*dsrE3C*)_BamHI_rev (Table S1) and cloned between the *NdeI* and *BamHI* sites of pET15b(+), resulting in pET15b-Hd-DsrE3C. Analogous procedures were followed for *dsrE3B* from *Thioalkalivibrio* sp. K90mix which was cloned between the *NdeI* and *BamHI* sites and *dsrE3B* from *Ts. sibirica* which was

cloned between the *XhoI* and *NdeI* sites generating the plasmids pET15b-TkDsrE3B and pET15b-TsDsrE3B. The *tusA* genes were amplified from *Hm. denitrificans*, *Thioalkalivibrio* sp. K90mix or *Ts. sibirica* genomic DNA with primers adding a sequence for a C-terminal Strep-tag and cloned between the *NdeI* and *EcoRI* sites of pET-22b(+). The *tusA* gene from *Aq. aeolicus* (aq_388a, coding for the protein WP_024015099.1) was amplified from genomic DNA with primers Aq388a_NdeI_fw and Aq388a_XhoI_rev (Table S1) introducing at the C-terminal position of the protein the two amino acids Leu and Glu directly followed by a 6xHis-tag, and cloned into the pET24a expression plasmid to generate the plasmid pET24a-AqTusA. Cysteine to serine exchanges were implemented to HdDsrE3C by SOE PCR using primers sets Hden0688_NdeI_fw and Hden0688_BamHI_rev, Hden0688_C83S_Fw, Hden0688_C83S_Rev and Hden0688_NdeI_fw and Hden0688_BamHI_rev, Hden0688_C84S_Fw, Hden0688_C84S_Rev, respectively, resulting in plasmids pET15b-DsrE3C-C83S and pET15b-DsrE3C-C84S. A cysteine to serine exchange was introduced into *Hm. denitrificans* TusA using the same method and the primers listed in Table S8. The Quik-Change Site-Directed Mutagenesis Kit (Stratagene) was used to generate the *Aq. aeolicus* *tusA* mutated genes (coding for AqTusA Cys¹⁷Ser and AqTusA Cys⁵⁴Ser) with the primers Aq388a_C17S_fw, Aq388a_C17S_rev and Aq388a_C54S_fw, Aq388a_C54S_rev using the pET24a-AqTusA plasmid.

Recombinant DsrE3B, DsrE3C, and TusA proteins were produced in *E. coli* BL21(DE3). Overnight precultures were used to inoculate fresh LB medium with a ratio of 1:50 (v/v). Synthesis of recombinant proteins was induced by the addition of 0.1 or 1 mM (for AqTusA) IPTG when cultures had reached an OD₆₀₀ of 0.6–0.8, followed by incubation for 2.5 h at 37°C. Cells were harvested by centrifugation (11,000 × g, 20 min, 4°C). Strep-tagged proteins were resuspended in 50 mM Tris–HCl buffer (pH 7.5) containing 150 mM NaCl. His-tagged proteins were resuspended in buffer containing 20 mM sodium-phosphate (20 mM Tris–HCl for AqTusA), 500 mM NaCl and 50 mM imidazole (pH 7.4). Cells were lysed by sonication (or with a cell disruptor for AqTusA). Insoluble cell material was subsequently removed by centrifugation (16,100 × g, 30 min, 4°C). His-tagged and Strep-tagged proteins were purified with Ni-NTA Agarose (Jena Bioscience, Jena, Germany) (except for AqTusA that was purified with a HiScreen Ni FF column (Cytiva, Freiburg, Germany)) and Strep-Tactin Superflow (IBA Lifesciences, Göttingen, Germany), respectively, according to the manufacturer's instructions. The proteins were then transferred to salt-free 50 mM Tris–HCl buffer (pH 7.5) or to 20 mM Tris–HCl buffer pH 7.4 for

AqTusA and stored at -70°C . Size exclusion chromatography on HiLoad 16/60 SuperdexTM 75 (Cytiva, Freiburg, Germany) was performed as described in Li, Törkel, et al. (2023).

5.6 | Protein–protein interaction in cell extracts

To detect interaction between AqTusA and DsrE-like proteins, TusA from *Aq. aeolicus* (200 μg) was incubated with crude soluble extract of *Aq. aeolicus* at room temperature and re-purified via His tag affinity-chromatography (HisTrap FF 1 mL column, Cytiva) according to the manufacturer's instructions. Soluble extracts were prepared as previously described (Boughanemi et al., 2020) except that cells were resuspended in 50 mM Tris–HCl, pH 7.3. Two different experiments were run: in the first one, purified AqTusA was incubated for 10 min with 500 μL of an extract obtained from cells grown with excess of hydrogen in the presence of thiosulfate (called 100% H_2) as described previously (Boughanemi et al., 2016); in the second trial, the protein was incubated for 30 min with 2 mL of extract prepared from cells grown with a lower amount of H_2 in the presence of thiosulfate (referred as 30% H_2 , condition in which the Hdr amount in cells is higher (Boughanemi et al., 2016)). In both cases, the AqTusA–extract mixtures were immediately frozen in liquid nitrogen after incubation and thawed just prior to purification. Proteins were eluted with a buffer containing 50 mM Tris–HCl pH 7.3, 150 mM NaCl, and 250 mM imidazole. A control experiment was run with the same extract but without TusA. After dialysis on a Vivaspin concentrator (molecular mass cutoff 3000 Da) with 50 mM Tris–HCl pH 7.3, eluted proteins from both columns underwent 18% SDS–PAGE or 15% Tris–Glycine native PAGE (without any reducing agent) (Guiral et al., 2009). Resulting bands were cut out of the gel and analyzed by LC–MS as described previously (Boughanemi et al., 2016). For the second experiment, total proteins in the elution fraction of the column were identified after the proteins were introduced in a 5% acrylamide stacking gel, as described in Prioretti et al. (2023) under the name “stacking method”. Protein concentrations were determined with the BCA protein assay kit from Sigma–Aldrich.

5.7 | Sulfur binding and transfer experiments

For sulfur binding experiments with the recombinant sulfur transferases from *Hm. denitrificans*, *Thioalkalivibrio* sp. K90mix, and *Ts. sibirica*, 1.5 nmol of the proteins were incubated with 5 mM polysulfide, thiosulfate,

tetrathionate, or GSSG in 20 μL 50 mM Tris–HCl, pH 7.5. The polysulfide stock solution needed for these experiments was prepared, diluted, and used as previously described (Ikeda et al., 1972; Li, Törkel, et al., 2023). For sulfur transfer experiments, 1.5 nmol of the putative sulfur-donating proteins were incubated with 0.5 mM polysulfide for 30 min at room temperature in 20 μL 50 mM Tris–HCl, pH 7.5. Acceptor proteins were reduced with 1 mM DTT under the same conditions. Excess of polysulfide or DTT was removed with micro Bio-Spin 6 columns (GE Healthcare, Munich, Germany) equilibrated with 50 mM Tris–HCl, pH 7.5. Efficient removal of polysulfide was confirmed by adding a filtered protein-free polysulfide solution to an acceptor protein, which was then tested for persulfidation via mass spectrometry. Donor and acceptor proteins were mixed in a 1:1 ratio to a final volume of 40 μL and incubated for 30 min at room temperature. The mixtures were then stored at -70°C . For mass spectrometry, samples of 20 μL were desalted by ZipTipC4 Pipette tips (Merck Millipore, Darmstadt, Germany), crystallized in a 2',6'-dihydroxyacetophenon matrix and measured by MALDI-TOF (matrix-assisted laser desorption ionization-time-of-flight) mass spectrometry at the Core Facility Protein Synthesis & BioAnalytics, Pharmaceutical Institute, University of Bonn.

For sulfur loading of AqTusA, 2 μg of protein was incubated for 30 min at 65°C , with 5 mM (final concentration) of the tested sulfur compound, in a final volume of 5 μL in 50 mM Tris–HCl pH 7.3. If reduction was desired, samples were incubated, with 10 mM DTT (final concentration) for 45 min at room temperature after the sulfur loading. Samples were immediately frozen in liquid nitrogen and stored at -80°C until further use. Before MALDI-TOF mass spectrometry analysis, the samples were desalted and concentrated with ZipTip C18 (Merck Millipore) using 0.1% trifluoroacetic acid (TFA) as desalting solution and 70% acetonitrile/0.1% TFA as elution solution. One microliter of samples (~ 41 pmol) mixed with 1 μL of matrix α -cyano-4-hydroxycinnamic acid were analyzed using the mass spectrometer Microflex II (Bruker). Three micrograms of AqTusA, incubated with cell extracts and re-purified on a HisTrap column (see Section 5.6), was diluted in 50 mM Tris–HCl pH 7.3 in a volume of 5 μL , desalted with ZipTipC18 and analyzed by MALDI-TOF as previously described (Guiral et al., 2009).

5.8 | Generation of datasets for phylogenetic and similarity network analyses

Archaeal and bacterial genomes were downloaded from Genome Taxonomy Database (GTDB, release R207). In

GTDB, all genomes are sorted according to validly published taxonomies, they are pre-validated and have high quality (completeness minus 5*contamination must be higher than 50%). One representative of each of the current 65,703 species clusters was analyzed. Open reading frames were determined using Prodigal (Hyatt et al., 2010) and subsequently annotated for sulfur related proteins via HMSS2 (Tanabe & Dahl, 2023). Annotation was extended by HMMs from TIGRFAMs (Li et al., 2021) and Pfam (Mistry et al., 2021) databases representing the 16 syntenic ribosomal proteins RpL2, 3, 4, 5, 6, 14, 15, 16, 18, 22, and 24, and RpS3, 8, 10, 17, and 19. A type I sHdr system was considered to be present if the core genes *shdrC1BIAHC2B2* were present in a syntenic gene cluster. For a type II sHdr system gene cluster *shdrC1BIAHB3* and *etfAB* had to be present in a single syntenic gene cluster (Cao et al., 2018; Justice et al., 2014).

5.9 | Phylogenetic tree inference and structural modeling

For phylogenetic tree inference, proteins were aligned using MAFFT (Kato & Standley, 2013) and trimmed with BMGE (Crisuolo & Gribaldo, 2010) (entropy threshold = 0.95, minimum length = 1, and matrix = BLOSUM30). Alignments were then used for maximum likelihood phylogeny inference using IQ-TREE v1.6.12 (Nguyen et al., 2015) implemented on the “bonna” high performance clusters of the University of Bonn. The best-fitting model of sequence evolution was selected using ModelFinder (Kalyaanamoorthy et al., 2017). Branch support was then calculated by SH-aLRT (2000 replicates) (Guindon et al., 2010), aBayes (2000 replicates) (Anisimova et al., 2011) and ultrafast bootstrap (2000 replicates) (Hoang et al., 2018). Finally, trees were displayed using iTol (Letunic & Bork, 2021). For species tree inference, results for each ribosomal protein were individually aligned, trimmed, and subsequently concatenated before they were used for phylogenetic tree construction. Structural models of proteins and protein complexes were generated using AlphaFold2 (Jumper et al., 2021).

5.10 | Sequence similarity network analysis

Amino acid sequences for the sequence similarity network were derived from the search of the GTDB dataset with HMSS2 (Tanabe & Dahl, 2023). Groups were chosen based on their sequence similarity and genomic context, which depended on the specific question being investigated. From all selected sequences a meaningful

and diverse set was derived via dereplication with mmseqs2 linclust (Steinegger & Söding, 2017) with default settings. Sequence similarity analysis was performed by an all versus all comparison with mmseqs2 search (Mirdita et al., 2019; Steinegger & Söding, 2017). The similarity matrix was modified in cytoscape and edges were filtered stepwise until optimal clustering was observed. This status was characterized as the minimum number of clusters while maintaining the highest number of connectivity within a group of annotated proteins, visualizing the grouping of proteins on a deep branching level.

AUTHOR CONTRIBUTIONS

Tomohisa Sebastian Tanabe: Conceptualization; investigation; writing – original draft; validation; writing – review and editing; visualization. **Elena Bach:** Investigation. **Giulia D’Ermo:** Investigation. **Marc Gregor Mohr:** Investigation. **Natalie Hager:** Investigation. **Niklas Pfeiffer:** Investigation. **Marianne Guiral:** Conceptualization; funding acquisition; validation; supervision; writing – review and editing; writing – original draft. **Christiane Dahl:** Conceptualization; funding acquisition; writing – original draft; writing – review and editing; project administration; supervision; formal analysis; validation; visualization.


ACKNOWLEDGMENTS


This work was funded by the Deutsche Forschungsgemeinschaft (Grant Da 351/13-1). Tomohisa Sebastian Tanabe received a scholarship from the Studienstiftung des Deutschen Volkes. We gratefully acknowledge the access to the Bonna HPC cluster hosted by the University of Bonn along with the support provided by its High Performance Computing & Analytics Lab. We gratefully thank for the support of France-Germany Hubert Curien Procope program for its exchange funding (n° 40444VM). We gratefully acknowledge the support of the Core Facility “Protein Synthesis and Bioanalytics” of the University of Bonn. The authors are also grateful to Régine Lebrun from the Core Facility “Protein Synthesis Mass spectrometry and Bioanalytics” proteomic platform of the University Mediterranean Institute of Microbiology (IMM) in Marseille (France), which is a part of the network “Marseille Protéomique”, IBiSA, and the Proteomic Platform IBiSA of the IMM, CNRS, Aix-Marseille Université for performing mass spectrometry. We thank Souhela Boughanemi and Robert van Lis (BIP-CNRS, Marseille) for *Aq. aeolicus tusA* cloning and site directed mutagenesis. We thank Alina Ballas for help with *Hm. denitrificans* growth experiments. Open Access funding enabled and organized by Projekt DEAL.

CONFLICT OF INTEREST STATEMENT

The authors declare no competing interests.

ORCID

Tomohisa Sebastian Tanabe  <https://orcid.org/0000-0003-2154-7980>

Christiane Dahl  <https://orcid.org/0000-0001-8288-7546>

REFERENCES

- Anisimova M, Gil M, Dufayard JF, Dessimoz C, Gascuel O. Survey of branch support methods demonstrates accuracy, power, and robustness of fast likelihood-based approximation schemes. *Syst Biol*. 2011;60:685–99.
- Atkinson HJ, Morris JH, Ferrin TE, Babbitt PC. Using sequence similarity networks for visualization of relationships across diverse protein superfamilies. *PLoS One*. 2009;4:e4345.
- Aussignargues C, Giuliani MC, Infossi P, Lojou E, Guiral M, Giudici-Orticoni MT, et al. Rhodanese functions as sulfur supplier for key enzymes in sulfur energy metabolism. *J Biol Chem*. 2012;287:19936–48.
- Ausubel FA, Brent R, Kingston RE, Moore DD, Seidman JG, Smith JA, et al. *Current protocols in molecular biology*. New York: John Wiley & Sons; 1997.
- Balleste-Delpierre C, Fernandez-Orth D, Ferrer-Navarro M, Diaz-Pena R, Odena-Caballo A, Oliveira E, et al. First insights into the pleiotropic role of *vrf* (*yedF*), a newly characterized gene of *Salmonella* Typhimurium. *Sci Rep*. 2017;7:15291.
- Bertani G. Lysogeny at mid-twentieth century: P1, P2, and other experimental systems. *J Bacteriol*. 2004;186:595–600.
- Bordo D, Bork P. The rhodanese/Cdc25 phosphatase superfamily—sequence–structure–function relations. *EMBO Rep*. 2002;3:741–6.
- Boughanemi S, Infossi P, Giudici-Orticoni MT, Schoepp-Cothenet B, Guiral M. Sulfite oxidation by the quinone-reducing molybdenum sulfite dehydrogenase SoeABC from the bacterium *Aquifex aeolicus*. *Biochim Biophys Acta Bioenerg*. 2020;1861:148279.
- Boughanemi S, Lyonnet J, Infossi P, Bauzan M, Kosta A, Lignon S, et al. Microbial oxidative sulfur metabolism: biochemical evidence of the membrane-bound heterodisulfide reductase-like complex of the bacterium *Aquifex aeolicus*. *FEMS Microbiol Lett*. 2016;363:fnw156.
- Bryantseva IA, Gorlenko VM, Kompantseva EI, Imhoff JF, Süling J, Mityushina L. *Thiorhodospira sibirica* gen. nov., sp. nov., a new alkaliphilic purple sulfur bacterium from a Siberian soda lake. *Int J Syst Bacteriol*. 1999;49:697–703.
- Cao X, Koch T, Steffens L, Finkensieper J, Ziggann R, Cronan JE, et al. Lipolate-binding proteins and specific lipolate-protein ligases in microbial sulfur oxidation reveal an atypical role for an old cofactor. *eLife*. 2018;7:e37439.
- Crisuolo A, Gribaldo S. BMGE (block mapping and gathering with entropy): a new software for selection of phylogenetic informative regions from multiple sequence alignments. *BMC Evol Biol*. 2010;10:210.
- Dahl C. Insertional gene inactivation in a phototrophic sulphur bacterium: APS-reductase-deficient mutants of *Chromatium vinosum*. *Microbiology*. 1996;142:3363–72.
- Dahl C. Cytoplasmic sulfur trafficking in sulfur-oxidizing prokaryotes. *IUBMB Life*. 2015;67:268–74.
- Dahl C. Sulfur metabolism in phototrophic bacteria. In: Hallenbeck PC, editor. *Modern topics in the phototrophic prokaryotes: metabolism, bioenergetics and omics*. Cham: Springer International Publishing; 2017. pp. 27–66.
- Dahl C. A biochemical view on the biological sulfur cycle. In: Lens P, editor. (2020) *Environmental technologies to treat sulfur pollution: principles and engineering*. IWA Publishing, London, pp. 55–96.
- Dahl JU, Radon C, Buhning M, Nimtz M, Leichert LI, Denis Y, et al. The sulfur carrier protein TusA has a pleiotropic role in *Escherichia coli* that also affects molybdenum cofactor biosynthesis. *J Biol Chem*. 2013;288:5426–42.
- Dahl C, Schulte A, Stockdreher Y, Hong C, Grimm F, Sander J, et al. Structural and molecular genetic insight into a widespread bacterial sulfur oxidation pathway. *J Mol Biol*. 2008;384:1287–300.
- Deckert G, Warren PV, Gaasterland T, Young WG, Lenox AL, Graham DE, et al. The complete genome of the hyperthermophilic bacterium *Aquifex aeolicus*. *Nature*. 1998;392:353–8.
- Ernst C, Kayashta K, Koch T, Venceslau SS, Pereira IAC, Demmer U, et al. Structural and spectroscopic characterization of a HdrA-like subunit from *Hyphomicrobium denitrificans*. *FEBS J*. 2021;288:1664–78.
- Geoghegan KF, Dixon HBF, Rosner PJ, Hoth LR, Lanzetti AJ, Borzilleri KA, et al. Spontaneous α -N-6-phosphogluconoylation of a “His Tag” in *Escherichia coli*: the cause of extra mass of 258 or 178 Da in fusion proteins. *Anal Biochem*. 1999;267:169–84.
- Gojon G. On H₂S prodrugs. *Antioxid Redox Signal*. 2020;33:999–1002.
- Guindon S, Dufayard JF, Lefort V, Anisimova M, Hordijk W, Gascuel O. New algorithms and methods to estimate maximum-likelihood phylogenies: assessing the performance of PhyML 3.0. *Syst Biol*. 2010;59:307–21.
- Guiral M, Prunetti L, Lignon S, Lebrun R, Moinier D, Giudici-Orticoni MT. New insights into the respiratory chains of the chemolithoautotrophic and hyperthermophilic bacterium *Aquifex aeolicus*. *J Proteome Res*. 2009;8:1717–30.
- Hallgren J, Tsirigios KD, Pedersen MD, Almagro Armenteros JJ, Marcatili P, Nielsen H, et al. DeepTMHMM predicts alpha and beta transmembrane proteins using deep neural networks. *bioRxiv*. 2022;04:04:08e487609. <https://doi.org/10.1101/2022.04.08.487609>
- Hoang DT, Chernomor O, von Haeseler A, Minh BQ, Vinh LS. UFBoot2: improving the ultrafast bootstrap approximation. *Mol Biol Evol*. 2018;35:518–22.
- Horton RM. PCR mediated recombination and mutagenesis: SOE-ing together tailor-made genes. *Mol Biotechnol*. 1995;3:93–99.
- Hug LA, Castelle CJ, Wrighton KC, Thomas BC, Sharon I, Frischkorn KR, et al. Community genomic analyses constrain the distribution of metabolic traits across the Chloroflexi phylum and indicate roles in sediment carbon cycling. *Microbiome*. 2013;1:22.
- Hyatt D, Chen GL, Locascio PF, Land ML, Larimer FW, Hauser LJ. Prodigal: prokaryotic gene recognition and translation initiation site identification. *BMC Bioinformatics*. 2010;11:119.
- Ikeda S, Satake H, Hisano T, Terazawa T. Potentiometric argentimetric method for the successive titration of sulphide and dissolved sulphur in polysulphide solutions. *Talanta*. 1972;19:1650–4.

- Ikei M, Miyazaki R, Monden K, Naito Y, Takeuchi A, Takahashi YS, et al. YeeD is an essential partner for YeeE-mediated thiosulfate uptake in bacteria and regulates thiosulfate ion decomposition. *PLoS Biol.* 2024;22(4):e3002601. <https://doi.org/10.1371/journal.pbio.3002601>
- Ikeuchi Y, Shigi N, Kato J, Nishimura A, Suzuki T. Mechanistic insights into sulfur relay by multiple sulfur mediators involved in thiouridine biosynthesis at tRNA wobble positions. *Mol Cell.* 2006;21:97–108.
- Ishii Y, Yamada H, Yamashino T, Ohashi K, Katoh E, Shindo H, et al. Deletion of the *yhhP* gene results in filamentous cell morphology in *Escherichia coli*. *Biosci Biotech Bioch.* 2000;64:799–807.
- Jaffe AL, Castelle CJ, Matheus Carnevali PB, Gribaldo S, Banfield JF. The rise of diversity in metabolic platforms across the candidate phyla radiation. *BMC Biol.* 2020;18:69.
- Jumper J, Evans R, Pritzel A, Green T, Figurnov M, Ronneberger O, et al. Highly accurate protein structure prediction with AlphaFold. *Nature.* 2021;596:583–9.
- Justice NB, Norman A, Brown CT, Singh A, Thomas BC, Banfield JF. Comparison of environmental and isolate *Sulfobacillus* genomes reveals diverse carbon, sulfur, nitrogen, and hydrogen metabolisms. *BMC Genomics.* 2014;15:1107.
- Kalyaanamoorthy S, Minh BQ, Wong TKF, von Haeseler A, Jermiin LS. ModelFinder: fast model selection for accurate phylogenetic estimates. *Nat Methods.* 2017;14:587–9.
- Katoh K, Standley DM. MAFFT multiple sequence alignment software version 7: improvements in performance and usability. *Mol Biol Evol.* 2013;30:772–80.
- Kessler D. Enzymatic activation of sulfur for incorporation into biomolecules in prokaryotes. *FEMS Microbiol Rev.* 2006;30:825–40.
- Koch T, Dahl C. A novel bacterial sulfur oxidation pathway provides a new link between the cycles of organic and inorganic sulfur compounds. *ISME J.* 2018;12:2479–91.
- Krishna SS, Tautz L, Xu Q, McMullan D, Miller MD, Abdubek P, et al. Crystal structure of NMA1982 from *Neisseria meningitidis* at 1.5 Å resolution provides a structural scaffold for nonclassical, eukaryotic-like phosphatases. *Proteins.* 2007;69:415–21.
- Kümpel C, Grosser M, Tanabe TS, Dahl C. Fe/S proteins in microbial sulfur oxidation. *Biochim Biophys Acta.* 2024;1871:119732.
- Letunic I, Bork P. Interactive Tree Of Life (iTOL) v5: an online tool for phylogenetic tree display and annotation. *Nucleic Acids Res.* 2021;49:W293–6.
- Li J, Koch J, Flegler W, Garcia Ruiz L, Hager N, Ballas A, et al. A metabolic puzzle: consumption of C₁ compounds and thiosulfate in *Hyphomicrobium denitrificans* X^T. *Biochim Biophys Acta Bioenerget.* 2023;1864:148932.
- Li W, O'Neill KR, Haft DH, DiCuccio M, Chetvernin V, Badretdin A, et al. RefSeq: expanding the prokaryotic genome annotation pipeline reach with protein family model curation. *Nucleic Acids Res.* 2021;49:D1020–8.
- Li J, Törkel K, Tanabe TS, Hsu HY, Dahl C. In the Alphaproteobacterium *Hyphomicrobium denitrificans* SoxR serves as a sulfane sulfur-responsive repressor of sulfur oxidation. *Antioxidants.* 2023;12:1620.
- Liu LJ, Stockdreher Y, Koch T, Sun ST, Fan Z, Josten M, et al. Thiosulfate transfer mediated by DsrE/TusA homologs from acidothermophilic sulfur-oxidizing archaeon *Metallosphaera cuprina*. *J Biol Chem.* 2014;289:26949–59.
- Liu LJ, You XY, Guo X, Liu SJ, Jiang CY. *Metallosphaera cuprina* sp. nov., an acidothermophilic, metal-mobilizing archaeon. *Int J Syst Evol Microbiol.* 2011;61:2395–400.
- Mirdita M, Steinegger M, Söding J. MMseqs2 desktop and local web server app for fast, interactive sequence searches. *Bioinformatics.* 2019;35:2856–8.
- Mistry J, Chuguransky S, Williams L, Qureshi M, Salazar GA, Sonnhammer ELL, et al. Pfam: the protein families database in 2021. *Nucleic Acids Res.* 2021;49:D412–9.
- Mueller EG. Trafficking in persulfides: delivering sulfur in biosynthetic pathways. *Nat Chem Biol.* 2006;2:185–94.
- Muyzer G, Sorokin DY, Mavromatis K, Lapidus A, Foster B, Sun H, et al. Complete genome sequence of *Thioalkalivibrio* sp. K90mix. *Stand Genomic Sci.* 2011;5:341–55. <https://doi.org/10.4056/sigs.2315092>
- Neukirchen S, Pereira IAC, Sousa FL. Stepwise pathway for early evolutionary assembly of dissimilatory sulfite and sulfate reduction. *ISME J.* 2023;17:1680–92.
- Nguyen LT, Schmidt HA, von Haeseler A, Minh BQ. IQ-TREE: a fast and effective stochastic algorithm for estimating maximum-likelihood phylogenies. *Mol Biol Evol.* 2015;32:268–74.
- Norris PR, Clark DA, Owen JP, Waterhouse S. Characteristics of *Sulfobacillus acidophilus* sp. nov. and other moderately thermophilic mineral-sulphide-oxidizing bacteria. *Microbiology.* 1996;142:775–83.
- Prioretti L, D'Ermo G, Infossi P, Kpebe A, Lebrun R, Bauzan M, et al. Carbon fixation in the chemolithoautotrophic bacterium *Aquifex aeolicus* involves two low-potential ferredoxins as partners of the PFOR and OGOR enzymes. *Life.* 2023;13:627.
- Ran M, Li Q, Xin Y, Ma S, Zhao R, Wang M, et al. Rhodanases minimize the accumulation of cellular sulfane sulfur to avoid disulfide stress during sulfide oxidation in bacteria. *Redox Biol.* 2022;53:102345.
- Ray WK, Zeng G, Potters MB, Mansuri AM, Larson TJ. Characterization of a 12-kilodalton rhodanese encoded by *glpE* of *Escherichia coli* and its interaction with thioredoxin. *J Bacteriol.* 2000;182:2277–84.
- Shi R, Proteau A, Villarroja M, Moukadiri I, Zhang LH, Trempe JF, et al. Structural basis for Fe–S cluster assembly and tRNA thiolation mediated by IscS protein–protein interactions. *PLoS Biol.* 2010;8:e1000354.
- Steinegger M, Söding J. MMseqs2 enables sensitive protein sequence searching for the analysis of massive data sets. *Nat Biotechnol.* 2017;35:1026–8.
- Stockdreher Y, Sturm M, Josten M, Sahl HG, Dobler N, Zigann R, et al. New proteins involved in sulfur trafficking in the cytoplasm of *Allochromatium vinosum*. *J Biol Chem.* 2014;289:12390–403.
- Stockdreher Y, Venceslau SS, Josten M, Sahl HG, Pereira IAC, Dahl C. Cytoplasmic sulfurtransferases in the purple sulfur bacterium *Allochromatium vinosum*: evidence for sulfur transfer from DsrEFH to DsrC. *PLoS One.* 2012;7:e40785.
- Szajli E, Feher T, Medzihradzky KF. Investigating the quantitative nature of MALDI-TOF MS. *Mol Cell Proteomics.* 2008;7:2410–8.

- Tanabe TS, Dahl C. HMS-S-S: a tool for the identification of sulphur metabolism-related genes and analysis of operon structures in genome and metagenome assemblies. *Mol Ecol Resour.* 2022; 22:2758–74.
- Tanabe TS, Dahl C. HMSS2: an advanced tool for the analysis of sulfur metabolism, including organosulfur compound transformation, in genome and metagenome assemblies. *Mol Ecol Resour.* 2023;23:1930–45.
- Tanabe TS, Grosser M, Hahn L, Kümpel C, Hartenfels H, Vtulkin E, et al. Identification of a novel lipoic acid biosynthesis pathway reveals the complex evolution of lipoate assembly in prokaryotes. *PLoS Biol.* 2023;21:e3002177.
- Tanabe TS, Leimkühler S, Dahl C. The functional diversity of the prokaryotic sulfur carrier protein TusA. *Adv Microb Physiol.* 2019;75:233–77.
- Tanaka Y, Yoshikaie K, Takeuchi A, Ichikawa M, Mori T, Uchino S, et al. Crystal structure of a YeeE/YedE family protein engaged in thiosulfate uptake. *Sci Adv.* 2020;6:eaba7637.
- Wagner T, Koch J, Ermler U, Shima S. Methanogenic heterodisulfide reductase (HdrABC-MvhAGD) uses two noncubane [4Fe-4S] clusters for reduction. *Science.* 2017;357:699–703.
- Watanabe T, Kojima H, Umezawa K, Hori C, Takasuka TE, Kato Y, et al. Genomes of neutrophilic sulfur-oxidizing chemolithoautotrophs representing 9 proteobacterial species from 8 genera. *Front Microbiol.* 2019;10:316.
- Westley J. Rhodanese. *Adv Enzymol Relat Areas Mol Biol.* 1973;39: 327–68.
- Xin Y, Liu H, Cui F, Liu H, Xun L. Recombinant *Escherichia coli* with sulfide:quinone oxidoreductase and persulfide dioxygenase rapidly oxidises sulfide to sulfite and thiosulfate via a new pathway. *Environ Microbiol.* 2016;18:5123–36.
- Yildiz T, Leimkühler S. TusA is a versatile protein that links translation efficiency to cell division in *Escherichia coli*. *J Bacteriol.* 2021;203(1):659–20.
- Zhang X, Liu X, Liang Y, Guo X, Xiao Y, Ma L, et al. Adaptive evolution of extreme acidophile *Sulfobacillus thermosulfidooxidans* potentially driven by horizontal gene transfer and gene loss. *Appl Environ Microbiol.* 2017;83:e03098–116.

SUPPORTING INFORMATION

Additional supporting information can be found online in the Supporting Information section at the end of this article.

How to cite this article: Tanabe TS, Bach E, D'Ermo G, Mohr MG, Hager N, Pfeiffer N, et al. A cascade of sulfur transferases delivers sulfur to the sulfur-oxidizing heterodisulfide reductase-like complex. *Protein Science.* 2024;33(6):e5014. <https://doi.org/10.1002/pro.5014>